UNIVERSITY OF CALIFORNIA
SANTA CRUZ

Regulation of Meiotic Synapsis in *C. elegans*

A dissertation submitted in partial satisfaction
of the requirements for the degree of

DOCTOR OF PHILOSOPHY

in

MOLECULAR, CELL, AND DEVELOPMENTAL BIOLOGY

by

Tisha Bohr

June 2016

The Dissertation of Tisha Bohr

Is approved:

_____
Professor Needhi Bhalla, Chair

_____
Professor Susan Strome

_____
Professor Bill Sullivan

_____
Tyrus Miller
Vice Provost and Dean of Graduate Studies

Table of Contents

List of Figures

Abstract

Regulation of Meiotic Synapsis in *C. elegans*

Tisha Bohr

Defects in chromosome segregation during cellular division can lead to daughter cells with the incorrect number of chromosomes. This is associated with cancer progression in mitotically dividing cells and birth defects and infertility in meiotically dividing cells. Therefore, cell cycle checkpoints are in place to monitor key events in order to reduce the probability of aberrant cell divisions. Synapsis involves the assembly of a proteinaceous structure, the synaptonemal complex (SC), between paired homologous chromosomes and is essential for proper meiotic chromosome segregation. In *C. elegans*, the synapsis checkpoint selectively removes nuclei with unsynapsed chromosomes. This checkpoint depends on Pairing Centers (PCs), *cis*- acting sites that promote pairing and synapsis by interacting with the nuclear envelope to access cytoplasmic microtubules. The spindle assembly checkpoint (SAC) monitors microtubule attachment at kinetochores during metaphase and also uses *cis*-acting sites, centromeres, as platforms for activation. These similarities led us to hypothesize that SAC proteins might also be required for the synapsis checkpoint. Here, I show that some SAC components are required to negatively regulate synapsis and promote the synapsis checkpoint response. These proteins require full PC function to inhibit synapsis, suggesting a role at PCs. These data support a model in which SAC proteins monitor the stability of pairing, between homologues to regulate synapsis and elicit a checkpoint response. I also show that SC components are required for a functional synapsis checkpoint. Mutation of these components does not abolish PC function, indicating they are bonafide checkpoint components. These data suggest that, in addition to homolog pairing, SC assembly may be monitored by the synapsis checkpoint. These findings are important in understanding conserved mechanisms that allow cells to maintain genomic integrity and lend insight into preventing human tumorigenesis, birth defects and infertility.

Acknowledgements

This dissertation is dedicated to Jack Dennis Bohr (1943-2013): dedicated father and lover of science.

I would like to thank my thesis advisor, Dr. Needhi Bhalla, for being such an extraordinarily thoughtful, engaged, and supportive advisor. I'm especially grateful for her willingness to allow me to explore my passion for teaching and diversity during my graduate career.

I'd like to thank all of the members of the Bhalla lab, past and present, who have made the lab such a fun and cohesive place to work in and for their helpful insights into my research. I'd like to thank Christian Nelson for performing the IPs in chapter 2 and for being an incredible friend and bay-mate during my time in the Bhalla lab. I'd like to thank Erin Klee, Guinevere Ashley, Evan Eggleston and Kyra Firestone for performing some apoptosis experiments in chapter 2 and 3 and for being incredibly dedicated undergraduate researchers and allowing me the opportunity to mentor them.

I'd like to thank my thesis committee members: Susan Strome and Bill Sullivan, for their support and valuable feedback on my research. I'd also like to thank Doug Kellogg for his time and advice as an ad-hoc committee member.

I would like to thank my beloved family; Uncle: Ron Bohr, Sisters: Tami Catalano and Teri Laguna, Soon to be Sister in Law: Nancy Le and loving mother: Trista McQueen; for all of their support and understanding. I would especially like to thank my incredibly supportive big brother, Jeremy Bohr, for always being there when I need him. He has always been my rock through this crazy thing called life. Last, but not least, I'm so incredibly grateful for my soon to be husband, Alex Baxter, who has amazingly supportive during my last couple years of graduate school. I'm so appreciative to him for standing by me as I follow my career across the country to New York state

Chapter 1: Introduction

Processes of Cellular Division

All organisms consist of cells and arise from preexisting cells, therefore cellular division is a fundamental requirement of life. Cell division is the process by which a parent cell divides into two or more daughter cells. In eukaryotes, there are two types of cell division. Mitosis is the cellular division process that generates genetically identical daughter cells through chromosome partitioning (Fig. 1-1). This division process is required for the proper development of all multicellular organisms, repair of tissues after injury or disease and organismal homeostasis. Successful mitosis requires that chromosomes first be replicated to produce identical sister chromatids. Mitotic cells then move through a number of stages where they condense and attach to the mitotic spindle to undergo one round of chromosome segregation followed by partitioning of the cytoplasm during cytokinesis. This process results in two genetically identical daughter cells (Fig. 1-1).

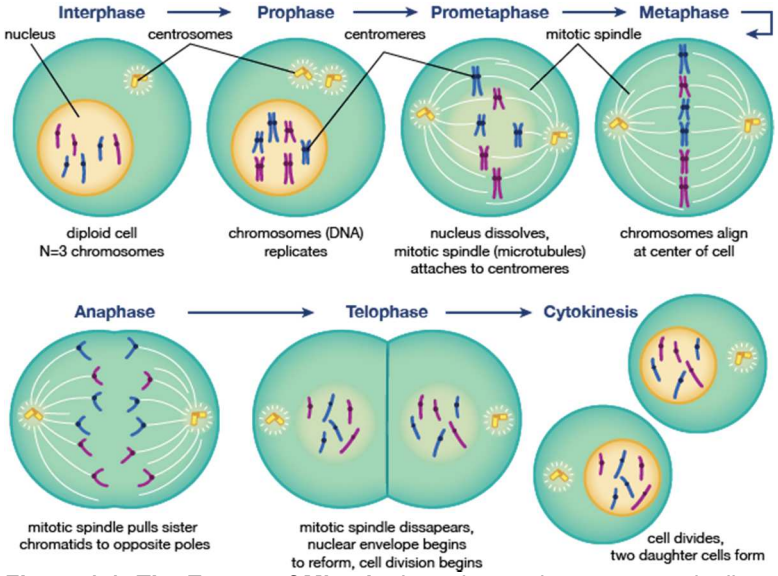

Figure 1-1: The Events of Mitosis. Interphase: chromosomes duplicate and remain attached to each other. Prophase: the chromosomes condense and become visible within the nucleus and the spindle forms in the cytoplasm. Prometaphase: the nuclear envelope breaks down, kinetochores form on each sister allowing the spindle to attach to centromeres. Metaphase: the copied chromosomes align (bi-orient) in the middle of the spindle (metaphase plate). Anaphase: sister chromatids are separated by the spindle into two genetically identical groups and moved to opposite ends of the spindle. Telophase: Nuclear membranes reform around each of the two sets of chromosomes. Chromosomes start to decondense and the spindle beings to break down. Cytokinesis: the cell splits into two daughter cells, each with the same number of chromosomes. (Cartoon acquired from Shmoop Editorial Team, 2008)

Meiosis is a specialized type of cell division that halves the amount of DNA in a cell to produce haploid gametes, such as eggs, sperm and pollen thus, is required for sexual reproduction. The meiotic process also allows for the shuffling of genetic information through recombination, which gives rise to novel combinations of alleles that underlie adaptation and natural selection. Meiosis produces haploid gametes by executing two successive chromosome segregation events after a single round of DNA replication (Fig. 1-2). In meiosis I a reductional division results in partitioning of homologous chromosomes. In meiosis II an equational division results in sister chromatids segregation in a way that is reminiscent of mitosis (Fig. 1-2).

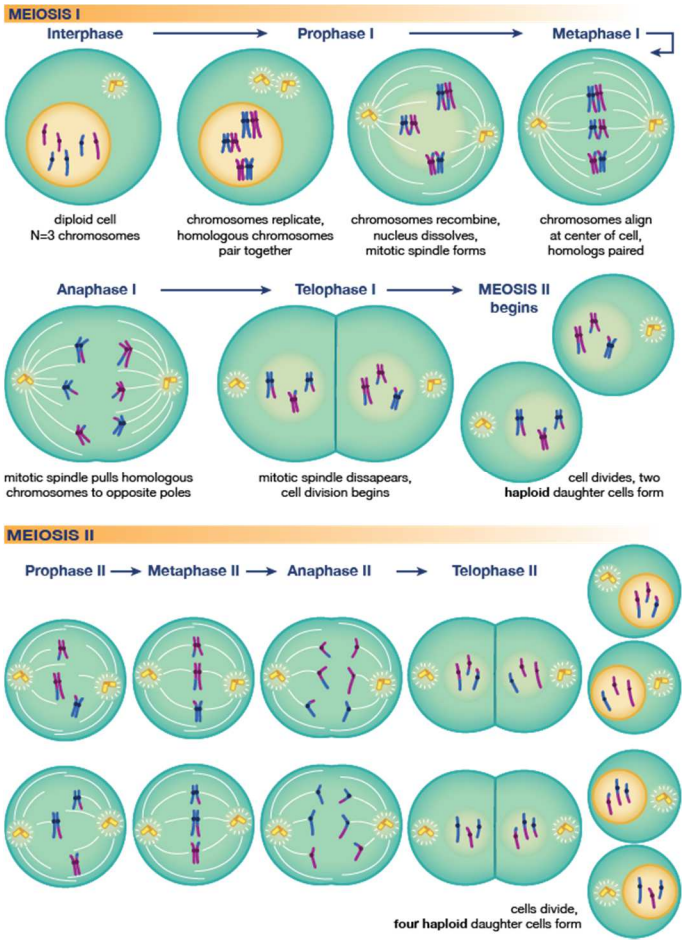

Figure 1-2: The Events of Meiosis. Interphase: chromosomes duplicate. Prophase I: the chromosomes condense and the spindle forms. Homologous chromosomes pair, synapses, and cross-over. Prometaphase I: the nuclear envelope breaks down, the kinetochore forms on the centromere of each homologue allowing spindle attachments. Metaphase I: homologous chromosomes align on the metaphase plate. The orientation is random, with either parental homologue on a side. Anaphase I: homologous chromosomes resolve their chiasmata and are separated by the spindle to opposite ends of the spindle. Telophase I: Nuclear membranes may reform or cells may move directly into meiosis II. Prophase II: centromeres on the sister chromatids attach to the spindle. Metaphase II: sister chromatids align in the middle of the spindle (metaphase plate). Anaphase II: sister chromatids are separated by the spindle into two genetically distinct groups and are moved to opposite ends of the spindle. Telophase II: Nuclear membranes reform. Cytokinesis: the cells split into daughter cells, each with the same number of chromosomes, half that of the original mother cells. (Cartoon acquired from Shmoop Editorial Team, 2008)

Chromosome Segregation and The Spindle Assembly Checkpoint

Successful cell division depends on accurate chromosome segregation to produce daughter cells with the correct chromosome complement. Improper chromosome segregation can lead to an abnormal number of chromosomes in daughter cells, termed aneiploidy. Zygotes that result from the fertilization of aneuploid gametes are typically inviable. In some cases, the inheritance of an extra chromosome is not lethal but can result in serious developmental disorders such as, Down, Turner's and Klinefelter's syndromes or cancer predisposition (Hassold and Hunt, 2001). Aneuploidy in mitotically dividing cells is associated with tumorigenesis and cancer progression (Gollin, 2005). Therefore, to ensure fidelity of chromosomes segregation, checkpoint mechanisms coordinate events during cell division. Events that are monitored by a checkpoint must be completed in a given amount of time or the checkpoint will not be satisfied, resulting in cell cycle arrest or cell death (apoptosis) (Murray, 1992). Either of these responses reduces the probability that the aberrant cell division will produce daughter cells with the incorrect number of chromosomes. Defects in cell cycle checkpoints have been linked to tumorigenesis, cancer progression birth defects and infertility (Gollin, 2005) making understanding these processes extremely relevant to human health issues.

In order to segregate successfully, chromosomes must interact with spindle microtubules. Spindle microtubules attach to chromosomes at epigenetically marked centromeric DNA regions (Cleveland et al., 2003). During mitosis and meiosis chromosomes build a hierarchical protein assembly called a kinetochore at the centromeric region, which links centromeric DNA to spindle microtubules, thereby coupling forces generated by microtubule dynamics to power chromosome movement (Cheeseman and Desai, 2008). Sister chromatids that attach to the spindle but do not bi-orient, or chromatids that lack spindle attachments altogether, are at risk for missegregation. Therefore, the spindle assembly checkpoint (SAC) monitors microtubule attachment and/or tension at kinetochores during metaphase and halts chromosome segregation until kinetochore-microtubule attachments

and bi-orientation are satisfied (Fig. 1-3) (Foley and Kapoor, 2013). The major components involved in the SAC were first identified in two, similar, genetic screens in budding yeast for mutants that fail to arrest in mitosis in the presence of microtubule-depolymerizing drugs, such as nacadazole. These checkpoint components were named Mad1, Mad2 and Mad3 (for mitotic arrest deficient) (Li and Murray, 1991), and Bub1 and Bub3 (for budding uninhibited by benzimidazole) (Hoyt et al., 1991). The SAC response and it's components are highly conserved. Homologs of many of these proteins have been identified in fission yeast (Bernard et al., 1998; He et al., 1997), *Xenopus* (Chen et al., 1998; Chen et al., 1996), *Drosophila* (Basu et al., 1999; Basu et al., 1998), *C. elegans* (Kitagawa and Rose, 1999), mice (Martinez-Exposito et al., 1999; Taylor et al., 1998) and humans (Cahill et al., 1998; Chan et al., 1999; Chan et al., 1998; Jin et al., 1998; Li and Benezra, 1996; Taylor et al., 1998). The high level of conservation of the SACs across organisms makes is an excellent mechanism to study in model organism for relevance to human health issues.

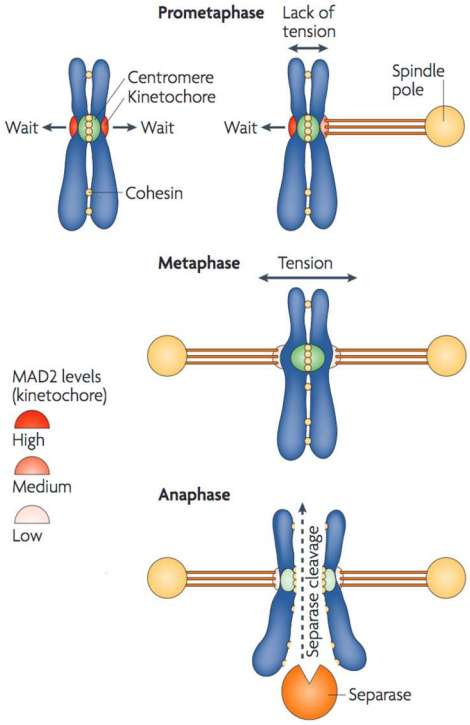

Figure 1-3: The Spindle Assembly Checkpoint. Unattached kinetochores generate a "wait anaphase" signal and recruit the spindle assembly checkpoint (SAC) proteins. The levels of Mad2 are high at unattached kinetochores (left) and moderately high at attached kinetochores in a monotelic pair (right). Bi-orientation depletes Mad2 (and other SAC components from kinetochores) and promotes the acquisition of tension in the centromere area. When all chromosomes have achieved this situation, the SAC signal is extinguished and anaphase ensues due to the activation of separase, which removes sister-chromatid cohesion by proteolysing cohesion. (cartoon modified from Musacchio and Salmon, 2007)

The SAC operates by recruiting factors, Mad1 and Mad2 and in some organisms Bub3 and Mad3/BubR1 to unattached kinetochores where a wait anaphase signal is generated. Localization of Mad1 and Mad2 and SAC function is also dependent on Bub1 which is localized to the kinetochore in a SAC independent manner (Murray, 1992; Musacchio and Salmon, 2007; Foley and Kapoor, 2013). Localization of the SAC

proteins to unattached kinetochores leads to the production of a complex called the mitotic checkpoint complex (MCC) that is comprised of Mad2, Mad3/BubR1 and Bub3. The MCC then interacts with and inhibits components of the anaphase promoting complex (APC) in order to halt chromosomes segregation until all chromosomes are properly bi-oriented. Once proper microtubule-kinetochore attachments are achieved, the signal is silence. This liberates the APC which degrades Securin. Degradation of Securin releases Seperase, which can then cleave sister chromatid cohesion allowing the chromosomes to separate and progress through anaphase (Fig. 1-3) (Murray, 1992; Musacchio and Salmon, 2007; Foley and Kapoor, 2013).

Early Meiotic Prophase and Chromosome Segregation

Defects in early meiotic prophase events can also lead to meiotic chromosome segregation defects during metaphase (Bhalla and Dernburg, 2008). In order to achieve proper meiotic chromosome segregation, homologous chromosomes must pair, synapsis and undergo cross-over recombination in early prophase. Recombination creates physical linkages, or chiasmata between homologues so that they can effectively b-iorient on the meiotic spindle (Fig. 1-4). In the absence of synapsis, crossover recombination is either completely abrogated or severely reduced (Bhalla and Dernburg, 2008), resulting in missegregation of meiotic chromosomes and aneuploid gametes that contribute to infertility and birth defects.

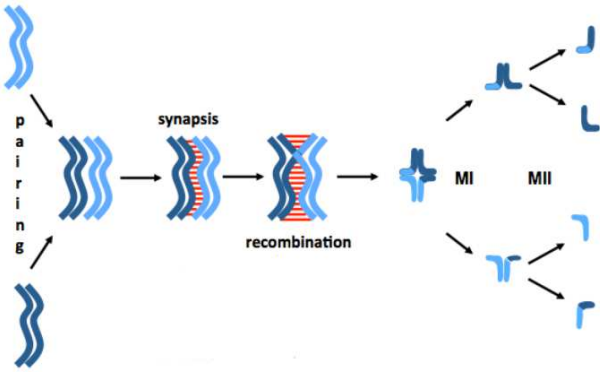

Figure1-4: The Events of Meiotic Prophase: Proper homolog segregation at meiosis I requires a physical linkage between homologous chromosomes called chiasma. The formation of chiasma depends on the events of meiotic prophase: pairing, synapsis, and crossover recombination. These processes are mediated by the synaptonemal complex, a proteinaceous structure that assembles between homologous chromosomes (shown in red).

In most organisms (e.g., plants, mammals, budding yeast, and filamentous fungi), recombination is mechanistically coupled to pairing and synapsis making it hard to distinguish between components that contribute to these different processes (Zickler and Kleckner, 2015). Recombination initiates by the introduction of programmed double-strand breaks (DSBs) in the G2/leptotene stage of prophase resulting in the linkages between homologous chromosomes. While a subset of these breaks will create cross-overs at the end of the pachytene stage of prophase, these interactions also typically mediate co-alignment of homologous chromosomes, to promote pairing. Following pairing, homologs become much more closely associated and stabilize these interactions by synapsis, in which a proteinaceous structure termed the synaptonemal complex (SC), assembles between each homologous pair. SC formation is usually nucleated at the sites of recombinational pairing interactions (Zickler and Kleckner, 2015).

In some organisms, the program of prophase events is somewhat different. For example, in female *Drosophila* and *C. elegans*, pairing and synapsis occur independently of recombination. (Lake and Hawley, 2012; Lui and Colaiacovo, 2013; Rog and Dernburg, 2013). Interestingly, with certain mutations, SC formation becomes dependent on recombination in *C. elegans* (Smolikov et al., 2008), highlighting that while these meiotic mechanisms function differently in different organisms there still seems to be conservation between how they operate. Regardless of how pairing, synapsis and recombination are coordinated, most organisms need all three of these mechanisms to be functional in order to carry out successful meiotic divisions.

Pairing and Synapsis

In many organisms, the onset of meiotic prophase is accompanied by a chromosome configuration in which chromosome ends associate with the NE, resulting in a roughly parallel alignment of the chromosome arms, particularly in regions near the telomeres leading to a

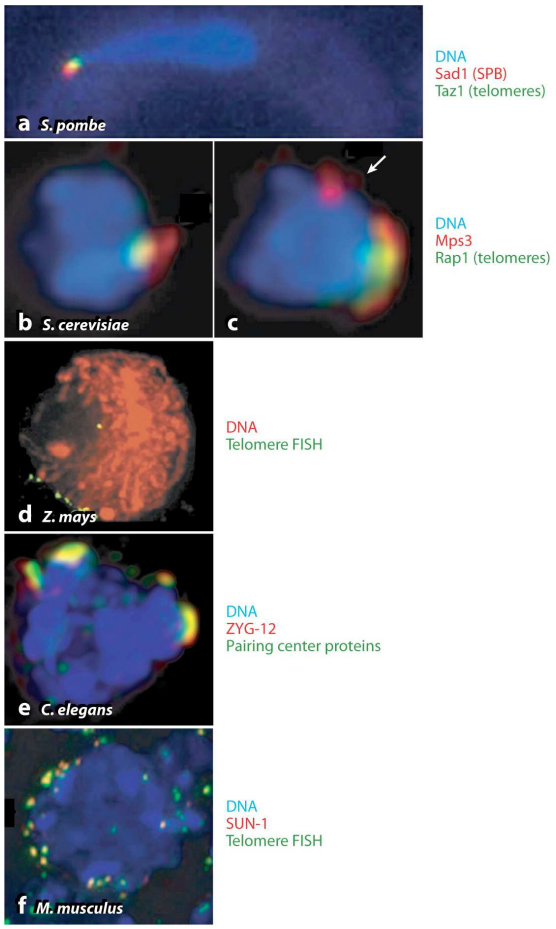

Figure1-5: Examples of meiotic chromosome attachment to the nuclear envelope. Images of pachytene nuclei in (*a*) *Schizosaccharomyces pombe*, (*b*,*c*) *Saccharomyces cerevisiae*, (*d*) *Zea mays*, (*e*) *Caenorhabditis elegans*, and (*f*) *Mus musculus*. The arrow in panel *c* indicates the spindle pole body. DNA is shown in blue, telomeres or chromosome ends are shown in green, and SUN (Sad1, Mps3, and SUN-1) or KASH (ZYG-12) domain proteins are indicated in red, except for in the *Z. mays* image, in which only the telomeres are shown. Images adapted from (Chikashige et al., 2006) (*a*), (Conrad et al., 2007) (*b*,*c*), (Bass et al., 1997) (*d*), and (Ding et al., 2007) (*f*)

clustered appearance of the chromatin (Fig. 1-5) (Bhalla and Dernburg, 2008). This reconfiguration of chromosome organization coincides with the onset of alignment, pairing, and synapsis, but it's contribution to these events is currently unknown. Genetic and cytological analysis has indicated that the stage associated with chromosome clustering involves three distinct but interdependent processes: chromosome NE attachment, clustering of chromosome ends, and cytoskeleton-facilitated chromosome movement. Each of these steps contributes to some aspects of proper homolog pairing. The degree of chromosome clustering between organisms varies from highly pronounced (Fig.1-5, a, c and b) to more subtly polarized (Fig. 1-5. c, d and e) (Bhalla and Dernburg, 2008). Therefore, chromosome attachment to the NE may play a more conserved and critical role in promoting chromosome pairing and synapsis by which simply typically results in the clustering of the chromosomes as a byproduct of this critical step.

Some components involved in meiotic chromosome NE attachment are clearly conserved throughout sexually reproducing species. SUN and KASH domain proteins are

transmembrane proteins that physically interact within the lumen of the NE between the inner and outer nuclear membranes (Fig. 1-5). The SUN domain protein (named for founding members Sad1 and UNC-84) usually extends into the nucleoplasm, whereas the KASH domain (named for Klarsicht/ANC-1/Syne homology) typically spans the outer NE into the cytoplasm. Pairs of SUN/KASH proteins link nuclear components to either the microtubule cytoskeleton or actin structures in the cytoplasm in a variety of cell types (Starr and Fischer, 2005). SUN/KASH proteins are also required for telomere attachment and synapsis in mice (Ding et al., 2007) and Sad1 and Kms1 are required for telomere clustering, synapsis and dynein interactions in *S. pombe* (Miki et al., 2002; Shimanuki et al., 1997; Yamamoto et al., 1999).

In *C. elegans* these SUN/KASH domain proteins play conserved roles in meiotic telomere attachment and homolog synapsis (Penkner et al. 2007; Sato, et. al., 2009). In *C. elegans*, SUN-1 interacts with the KASH domain protein ZYG- 12 to link chromosomes to microtubules and cytoplasmic dynein (Penkner et al., 2007; Sato et al., 2009). These chromosome NE attachments are mediate through specific sites located near one end of each chromosome, termed pairing centers (PCs) (Lui and Colaiacovo, 2013; Rog and Dernburg, 2013; Tsai and McKee, 2011). PCs are comprised of complex arrays of DNA repeat sequences bound by zinc-finger (ZnF) proteins (MacQueen et al., 2005; Phillips and Dernburg, 2006; Phillips et al., 2005). PCs and their ZnF binding proteins are not only required for meiotic chromosome NE attachment are also required for pairing and synapsis (Sato et al., 2009) and act as the the sites of synapsis initiation (Rog and Dernburg, 2015). Interestingly, PCs are not sufficient for homology assessment (Sato et al., 2009), implying that mechanisms involved in and synapsis are distinct from assessing homology in *C. elegans*.

Synapsis requires that axial elements assemble between replicated sister chromatids to support homolog pairing. In most species, axial elements consist of HORMA domain proteins (HORMADs) (Hollingsworth et al., 1990) (Aravind and Koonin, 1998) (Caryl et al., 2000) (Fukuda et al., 2010) (Wojtasz et al., 2009). In *C. elegans*, four HORMAD proteins, HTP-3,

HIM-3, HTP-1, and HTP-2, comprise the axial elements of the SC and play overlapping but distinct roles during meiotic prophase (Zetka et al., 1999) (Couteau et al., 2004) (Couteau and Zetka, 2005) (Martinez-Perez and Villeneuve, 2005) (Goodyer et al., 2008). Synapsis is complete when the central element of the SC is assembled between paired axial elements of homologous chromosomes (Fig 1-6). In *C. elegans*, the central element includes the factors SYP-1, SYP-2, SYP-3 and SYP-4 (MacQueen et al., 2002) (Colaiacovo et al., 2003) (Smolikov et al., 2007) (Smolikov et al., 2009).

The structure of the central elements are as evolutionarily conserved as meiosis itself. However, while it's components share a common underlying structural organization across phyla, the level of their primary amino acid sequence homology is very low. Therefore it has been commonly thought that these molecules play primarily structural roles, rather than catalytic ones (Fraune et al., 2012; Mercier and Grelon, 2008; Page and Hawley, 2004; Schild-Prufert et al., 2011; Wojtasz et al., 2009; Yang and Wang, 2009). We are only beginning to understand how SC axial and central elements interact to form the SC, how they are regulated as well as what other undefined roles they may have.

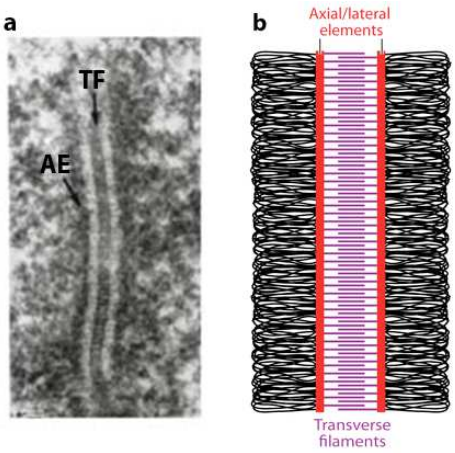

Figure 1-6: The Synaptonemal Complex. (**a**) Electronic microscope (Cheeseman and Desai) of longitudinal section of *Blaps cribrosa* synaptonemal complex with distinct central region transverse filaments which appears as a zipper-like structure flanked by electron-dense patches of chromatin (Adapted from (Schmekel, 1993 #41)) (**b**) Schematic of the synaptonemal complex. The axial/lateral elements (**red**) assemble between sister chromatids prior to or concomitant with pairing. The transverse filaments/central elements (**purple**) polymerize between paired homologs to complete synapsis. (adapted from Bhalla and Dernburg, 2008).

The Synapsis Checkpoint

Defects in these early meiotic events can lead to cell cycle arrest or apoptosis, indicating that the events are monitored by checkpoints. In budding yeast, a pachytene checkpoint responds to defects in homolog synapsis and/or recombination (Roeder and Bailis, 2000).

Mammalian meiosis may have two distinct checkpoints, one that responds to synaptic failure and one that responds to DNA damage (Baudat et al., 2000; Di Giacomo et al., 2005; Odorisio et al., 1998). Because synapsis and recombination are mechanistically coupled in both budding yeast (Giroux et al., 1989) and mice (Baudat et al., 2000; Romanienko and Camerini-Otero, 2000), it has been ambiguous whether these checkpoints are triggered by recombination defects or asynapsis.

In *C. elegans*, unsynapsed chromosomes activate germline apoptosis independently of a DNA damage checkpoint that monitors recombination (Bhalla and Dernburg, 2005; Dernburg et al., 1998; MacQueen and Hochwagen, 2011). This indicates that a distinct checkpoint monitors unsynapsed chromosomes in meiosis. This feature of *C. elegans* allows us to uniquely identify genes that are specifically required for the synapsis checkpoint, a task that has been difficult to do in other organisms in which synapsis and recombination are coupled.

Linking Pairing Centers and Centromeres

Despite their functional differences, PCs have been compared to centromeres (Dernburg, 2001; Labella et al., 2011). For example, in a holocentric organism such as *C. elegans*, deleterious chromosome rearrangements can be transmitted mitotically (Albertson et al., 1997). By limiting synapsis initiation to a single site per chromosome, PCs may contribute to karyotype stability during meiosis in a manner similar to point centromeres during chromosome segregation (Albertson et al., 1997; Dernburg, 2001; MacQueen et al., 2005). More importantly, centromeres and PCs are both specialized *cis*-acting chromosomal sites

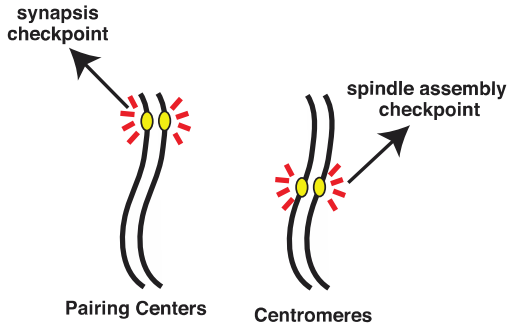

Figure 1-7: Comparison of Pairing Centers and Centromeres. Both Pairing Centers (yellow, left) and centromeres (yellow, right) are *cis*-acting cites that act as platforms for checkpoint activation. Pairing Centers are required for the synapsis checkpoint and centromeres are required for the spindle assembly checkpoint. Both Pairing Centers and centromeres building protein structures that interact with microtubules in order to facilitate chromosome dynamics.

that nucleate transient structures to mediate microtubule binding, promote specific chromosome behavior and generate a checkpoint response (Fig. 1-7). During metaphase, centromeres assemble kinetochores to orchestrate chromosome segregation (Cheeseman and Desai, 2008) and regulate the SAC (Foley and Kapoor, 2013). During prophase, PCs recruit Znf proteins in order to regulate chromosome dynamics to orchestrate pairing and synapsis and promote the synapsis checkpoint (Bhalla and Dernburg, 2005; Phillips and Dernburg, 2006; Phillips et al., 2005; Sato et al., 2009). In addition, like PCs (Rog and Dernburg, 2015), centromeres can act as sites for meiotic synapsis initiation in budding yeast (Tsubouchi et al., 2008; Tsubouchi and Roeder, 2005) and *Drosophila* (Takeo et al., 2011; Tanneti et al., 2011). The similarities between these *cis*-acting sequences and their involvement in monitoring events they participate in may reflect aspects of the evolutionary relationship between centromeres and PCs.

Chapter 2: Spindle assembly checkpoint proteins regulate and monitor meiotic synapsis in *C. elegans*

Introduction

Cell cycle checkpoints ensure accurate chromosome segregation by monitoring the progression of critical events (Murray, 1992). When errors occur, checkpoints prevent the production of aneuploid daughter cells by either arresting the cell cycle to promote error correction or targeting the cell for apoptosis. Aneuploidy is a hallmark of tumor cells undergoing mitosis (Kops et al., 2005) and is associated with birth defects and infertility during sexual reproduction (Hassold and Hunt, 2001).

Sexual reproduction requires meiosis, a specialized cell division that produces gametes such as eggs and sperm. During meiotic prophase, homologous chromosomes pair and synapse to undergo crossover recombination, a prerequisite for proper meiotic chromosome segregation (Bhalla and Dernburg, 2008). In *Caenorhabditis elegans*, the synapsis checkpoint induces apoptosis to remove nuclei with unsynapsed chromosomes (Bhalla and Dernburg, 2005). This checkpoint depends on cis-acting sites near one end of each chromosome termed pairing centers (PCs; Bhalla and Dernburg, 2005), which are also essential for pairing and synapsis (MacQueen et al., 2005). Early in meiotic prophase PCs recruit factors, such as HIM-8, ZIM-1, ZIM-2, and ZIM-3 (Phillips et al., 2005; Phillips and Dernburg, 2006), to assemble a transient regulatory platform that interacts with the conserved nuclear envelope proteins SUN-1 and ZYG-12. This interaction allows PCs access to the cytoplasmic microtubule network and the microtubule-associated motor, dynein (Penkner et al., 2007; Sato et al., 2009; Labrador et al., 2013). The mobilization of chromosomes by cytoskeletal forces is a conserved feature of meiotic prophase (Bhalla and Dernburg, 2008) that facilitates homologue pairing and synapsis (Sato et al., 2009; Labrador et al., 2013).

When dynein function is abolished, chromosomes pair but fail to synapse (Sato et al., 2009). These data have led to a working model in which dynein is dispensable for homologue pairing but licenses synapsis through a tension-sensing mechanism (Sato et al., 2009;

Wynne et al., 2012). This model proposes that when a chromosome identifies its homologue and remains stably paired, it resists the pulling forces of dynein. This resistance, or tension, is thought to initiate synapsis at PCs. However, if nonhomologous chromosomes interact, they cannot resist dynein's pulling forces and restart the homology search. How tension between PCs could be monitored to regulate synapsis is unknown.

Despite their functional differences, PCs have been compared with centromeres (Dernburg, 2001; Labella et al., 2011). Both are cis-acting chromosomal sites that nucleate transient structures to mediate microtubule binding, promote specific chromosome behavior, and generate a checkpoint response. In addition, centromeres can act as sites for meiotic synapsis initiation in budding yeast (Tsubouchi and Roeder, 2005; Tsubouchi et al., 2008) and *Drosophila* (Takeo et al., 2011; Tanneti et al., 2011). Centromeres assemble kinetochores to orchestrate chromosome segregation (Cheeseman and Desai, 2008). Kinetochores also provide a platform for the spindle assembly checkpoint (SAC), which inhibits the anaphase-promoting complex (APC) and halts cell cycle progression until all kinetochores are successfully bioriented (Foley and Kapoor, 2013). Because of the similarities between PCs and centromeres, we hypothesized that components of the SAC might act at PCs during meiotic prophase. We report that MAD-1, MAD-2, and BUB-3 are required for the synapsis checkpoint and negatively regulate synapsis in *C. elegans*. Mutation of *mad-1*, *mad-2*, or *bub-3* suppresses synapsis defects in dynein mutants, implicating SAC components in the tension-sensing mechanism that is thought to license meiotic synapsis. These roles in monitoring and regulating synapsis are independent of a conserved APC component, indicating MAD-1, MAD-2, and BUB-3 are performing a role aside from inhibiting the APC. MAD-1 and MAD-2 localize to the nuclear periphery and coimmunoprecipitate with SUN-1. Furthermore, MAD-1 and BUB-3 require full PC function to inhibit synapsis. Altogether, these data strongly suggest that SAC proteins function at PCs. Therefore, we propose that the ability of some SAC components to monitor tension is conserved and may have been coopted in a variety of biological contexts to maintain genomic integrity.

Results and Discussion

MAD-1, MAD-2, and BUB-3 are required for the synapsis checkpoint

To determine whether SAC proteins are required for the synapsis checkpoint, we used a hypomorphic allele of *mad-1* (*mdf-1[av19]*) defective in SAC function (Stein et al., 2007; Yamamoto et al., 2008) and null mutations of three core but nonessential SAC components, *mad-2Δ*, *mad-3Δ* (known as *mdf-2* and *mdf-3/san-1*, respectively, in *C. elegans*), and *bub-3Δ* (Kitagawa and Rose, 1999; Essex et al., 2009). We refer to the *mad-1(av19)* allele as *mad-1(cd)* for checkpoint deficient. *meDf2* is a deficiency that removes the X chromosome PC (Villeneuve, 1994). Animals heterozygous for *meDf2* (*meDf2/+*) have unsynapsed X

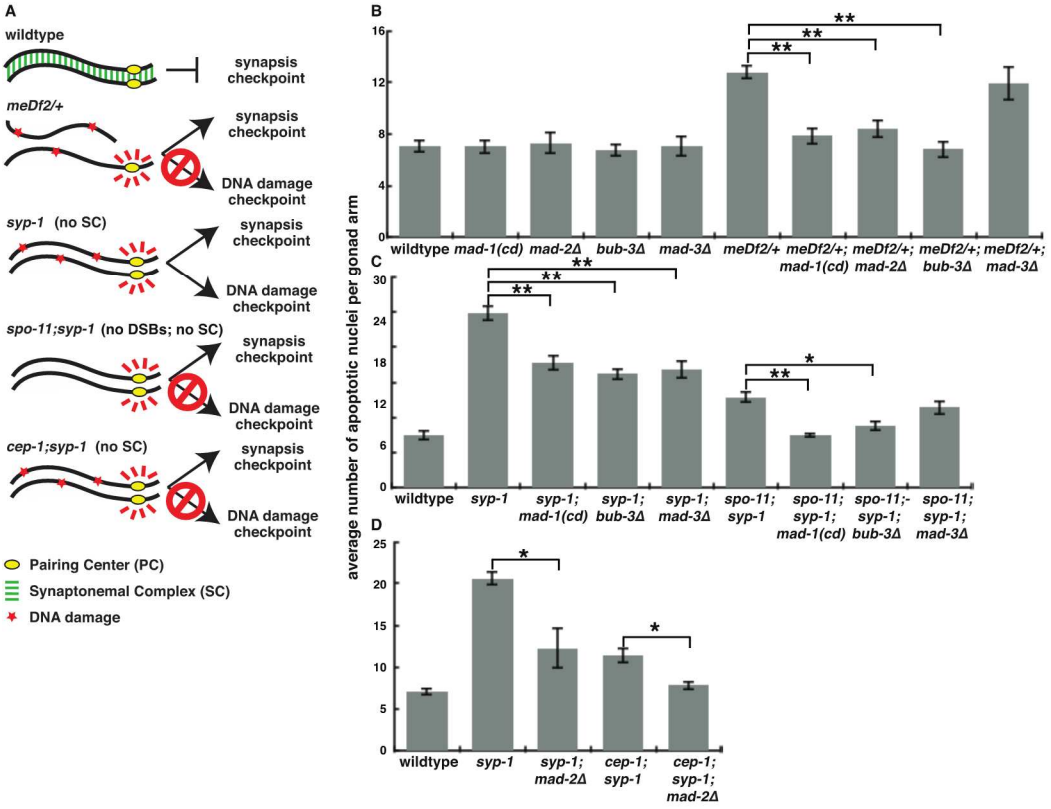

Figure 2-1: MAD-1, MAD-2, and BUB-3 are required for the synapsis checkpoint. (A) Meiotic checkpoints in *C. elegans*. (B) Mutation of *mad-1*, *mad-2*, or *bub-3*, but not *mad-3,* reduces germline apoptosis in *meDf2/+*. (C) Mutation of *mad-1* or *bub-3* reduces germline apoptosis in *syp-1* and *spo-11;syp-1* mutants, whereas mutation of *mad-3* reduces apoptosis in *syp-1* but not in *spo-11;syp-1* mutants. (D) Mutation of *mad-2* reduces germline apoptosis in *syp-1* and *cep-1;syp-1* mutants. Error bars represent ±SEM. *, P < 0.01; **, P < 0.0001.

chromosomes in a subset of meiotic nuclei because synapsis cannot initiate efficiently (MacQueen et al., 2005). The synapsis checkpoint responds to these unsynapsed chromosomes by elevating germline apoptosis above wild-type physiological levels (Fig. 2-1, A and B; Bhalla and Dernburg, 2005). We introduced SAC mutations into *meDf2/+* and found that loss of *mad-1*, *mad-2*, or *bub-3*, but not *mad-3*, decreased apoptosis in *meDf2/+* to wild type levels (Fig. 2-1 B), illustrating that MAD-1, MAD-2, and BUB-3 are required for the synapsis checkpoint when X chromosomes are unsynapsed.

meDf2 homozygotes exhibit asynapsis in almost all meiotic nuclei (MacQueen et al., 2005). However, these mutant worms exhibit elevated germline apoptosis as the result of the DNA damage checkpoint (Fig. 2-2, A and B) because functional PCs are required for the synapsis checkpoint (Bhalla and Dernburg, 2005). Mutation of *mad-1*, *mad-2*, *mad-3*, or *bub-3* did not reduce apoptosis in *meDf2* homozygotes (Fig. 2-2 B). Therefore, MAD-1, MAD-2, and BUB-3 are specifically required to induce germline apoptosis in response to the synapsis checkpoint.

Next, we tested the requirement for SAC components in the synapsis checkpoint when all chromosomes are unsynapsed. Synapsis requires the assembly of the synaptonemal complex (SC) between homologous chromosomes (Bhalla and Dernburg, 2008). *syp-1* mutants do not load SCs between homologues (MacQueen et al., 2002), leading to high levels of checkpoint-induced germline apoptosis as a result of both the synapsis and DNA damage checkpoints (Fig. 2-1, A, C, and D; Bhalla and Dernburg, 2005). Mutation of *mad-1*, *mad-2*, *mad-3*, or *bub-3* in the *syp-1* mutant background reduced apoptosis to intermediate levels, indicating loss of one checkpoint but not both (Fig. 2-1, C and D).

To determine which checkpoint these genes are required for, we prevented the DNA damage checkpoint response in *syp-1* mutants by mutating either *spo-11* or *cep-1* (Fig. 2-1 A; Bhalla and Dernburg, 2005). SPO-11 generates double-strand breaks that initiate meiotic recombination (Dernburg et al., 1998), and CEP-1 (the *C. elegans* p53 orthologue) promotes germline apoptosis in response to DNA damage (Derry et al., 2001; Schumacher et al.,

2001). Therefore, the elevated apoptosis in *spo-11;syp-1* and *cep-1;syp-1* double mutants is solely a consequence of the synapsis checkpoint (Fig. 2-1 A; Bhalla and Dernburg, 2005). Mutation of *mad-1* or *bub-3* in the *spo-11;syp-1* background or *mad-2* in the *cep-1;syp-1*

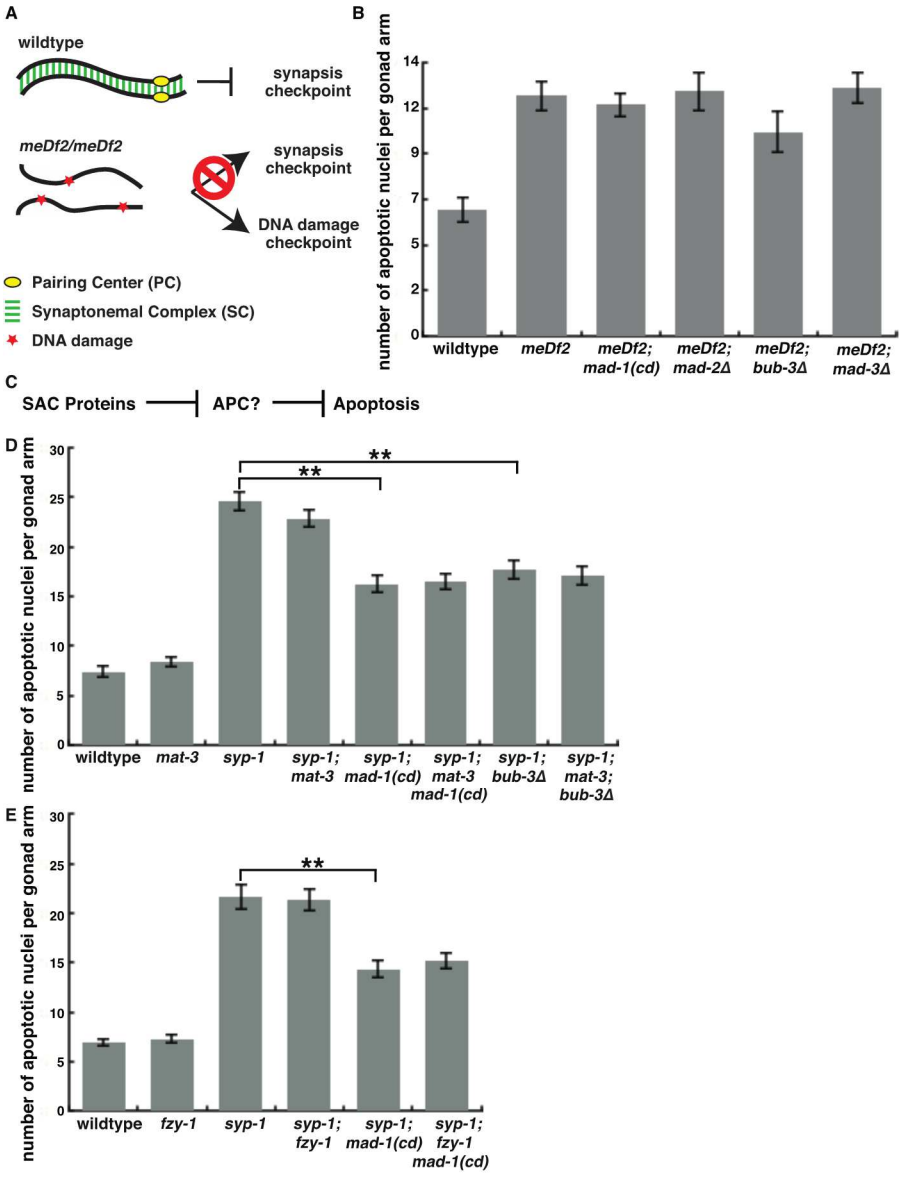

Figure 2-2: SAC components MAD-1, MAD-2, and BUB-3 are not required for the DNA damage checkpoint, and loss of APC components does not affect the synapsis checkpoint. (A) DNA damage checkpoint response in *meDf2* homozygotes. (B) Mutations in *mad-1*, *mad-2*, or *bub-3* do not affect apoptosis in *meDf2* homozygotes. (C) Schematic of the possible role of the APC in the synapsis checkpoint. (D) Mutation of *mat-3* does not affect germline apoptosis in *syp-1*, *syp-1;mad-1(cd)*, or *syp-1;bub-3Δ* mutants. (E) Mutation of *fzy-1* does not affect germline apoptosis in *syp-1*or *syp-1;mad-1(cd)* mutants. Error bars represent ±SEM. **, P < 0.0001

background produced wild-type levels of apoptosis (Fig. 2-1, C and D). However, mutation of *mad-3* in *spo-11;syp-1* mutants did not further decrease apoptosis (Fig. 2-1 C), suggesting that MAD-3 is required for the DNA damage checkpoint in *syp-1* mutants. Because this differs from our results with *meDf2;mad-3Δ* double mutants (Fig. 2-2 B), we infer that the DNA damage checkpoint responds differently if all chromosomes are unsynapsed (*syp-1* mutants) versus if one pair of chromosomes are unsynapsed (*meDf2* mutants). More importantly, these data establish that MAD-1, MAD-2, and BUB-3, but not MAD-3, are required for the synapsis checkpoint when all chromosomes are unsynapsed.

Mad2, Bub3, and Mad3 form the mitotic checkpoint complex (MCC), which inhibits the APC activator Cdc20 and entry into anaphase (Sudakin et al., 2001). MAD-3's primary role during the SAC response may be inhibition of the APC (Shonn et al., 2003), suggesting that the APC might also not be involved in the synapsis checkpoint. To test this, we used a temperature-sensitive allele of *mat-3*, the orthologue of Cdc23/Apc8 and an essential subunit of the APC (Golden et al., 2000). We predicted that if SAC components were acting through the APC, loss of APC activity would elevate germline apoptosis as the result of an inappropriate checkpoint response (Fig. 2-2 C). However, germline apoptosis in *mat-3*, *syp-1;mat-3;mad-1(cd)*, or *syp-1;mat-3;bub-3Δ* mutants was unaffected in comparison with wild-type, *syp-1;mad-1(cd)*, and *syp-1;bub-3Δ* backgrounds, respectively (Fig. 2-2 D). We also evaluated whether Cdc20 (FZY-1 in *C. elegans*) was involved in the synapsis checkpoint using a loss of function allele (Kitagawa et al., 2002) but detected no change in apoptosis in *fzy-1* or *syp-1;fzy-1;mad-1(cd)* mutants when compared with wild-type or *syp-1;mad-1(cd)* worms, respectively (Fig. 2-2 E). Together these data indicate that the APC is unlikely to be the target of SAC components in the synapsis checkpoint. Intriguingly, orthologues of some SAC components, but not APC components, have been identified in the *Giardia* genome (Gourguechon et al., 2013). Loss of these conserved SAC components produces chromosome segregation errors (Vicente and Cande, 2014), suggesting that they may have additional roles in regulating chromosome behavior.

In addition to the synapsis checkpoint, asynapsis is associated with a delay in meiotic progression in which chromosomes remain asymmetrically localized (clustered) in meiotic nuclei (Fig. 2-3 A; MacQueen et al., 2002). To evaluate whether SAC proteins affect meiotic progression, we quantified the percentage of nuclei in which chromosomes appeared clustered (Fig. 2-3, B and C). *mad-1(cd)* and *bub-3Δ* mutants had slightly more nuclei with clustered chromosomes than wild-type germlines, suggesting defects in synapsis or recombination (Fig. 2-3, B and C). However, neither of the single mutants exhibited any achiasmate chromosomes (not depicted), indicating that crossover recombination is not

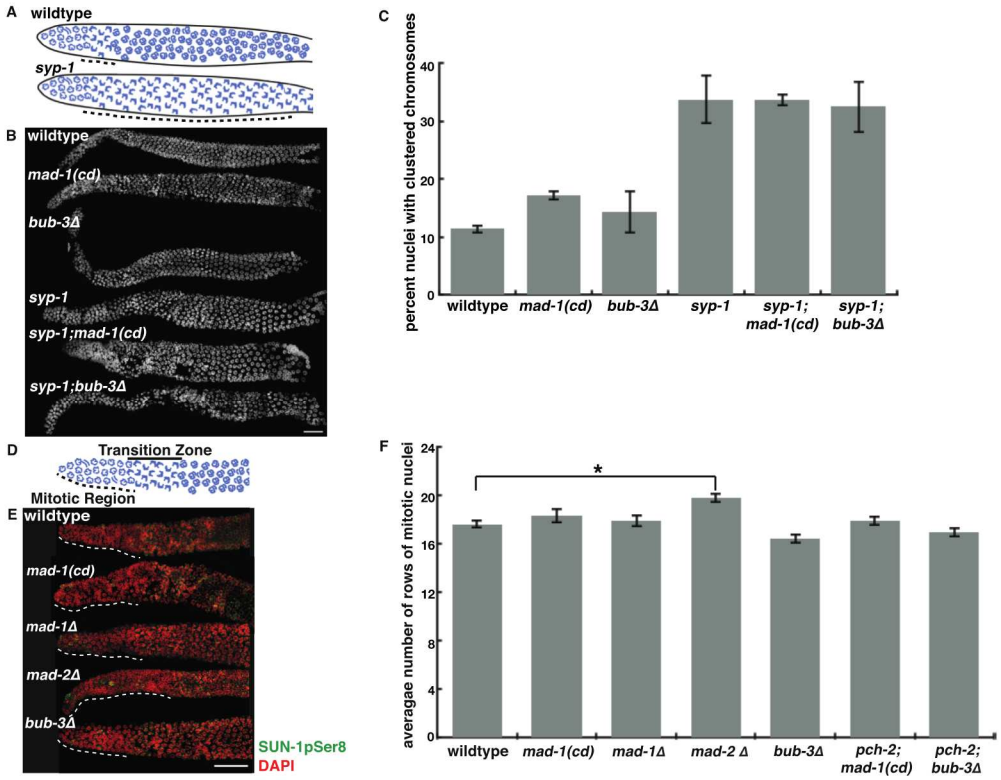

Figure 2-3: Loss of MAD-1 or BUB-3 does not affect meiotic entry or meiotic progression. (A) Cartoon depicts wild-type and *syp-1* germlines. (B) Images of wild-type, *mad-1(cd)*, *bub-3Δ*, *syp-1*, *syp-1;mad-1(cd)*, and *syp-1;bub-3Δ* germlines stained with DAPI. Regions of clustered chromosomes are indicated by dashed lines. (C) Mutation of *mad-1* and *bub-3* results in slightly more nuclei with clustered chromosomes than wild-type germlines but does not reduce the percentage of nuclei with clustered chromosomes in *syp-1* mutants. (D) Cartoon depicts mitotic and early meiotic region (transition zone) of the germline. (E) Images of the mitotic and early meiotic region of germlines in wild-type, *mad-1(cd)*, *mad-1Δ*, *mad-2Δ*, and *bub-3Δ* mutants stained with DAPI and an antibody against SUN-1pSer8. The length of the mitotic region is indicated by dashed lines. (F) *mad-2Δ* delays meiotic entry, whereas *mad-1(cd)*, *mad-1Δ*, *bub-3Δ*, *pch-2;mad-1(cd)*, and *pch-2;bub-3Δ* double mutants do not affect meiotic entry. Bars, 30 μm. Error bars represent ±SEM. *, $P < 0.01$; **, $P < 0.0001$

disrupted. More importantly, we did not detect any difference in the percentage of nuclei with clustered chromosomes between *syp-1;mad-1(cd)* or *syp-1;bub-3Δ* double mutants and *syp-1* single mutants (Fig. 2-3, B and C). Therefore, MAD-1 and BUB-3 are specifically required for the synapsis checkpoint and not for the delay in meiotic progression that accompanies asynapsis.

MAD-1 and MAD-2 interact with SUN-1 and localize to the periphery of meiotic nuclei

SAC components localize to unattached kinetochores to initiate checkpoint signaling (Foley and Kapoor, 2013). In meiotic prophase, SUN-1 is present at the nuclear periphery and colocalizes with PCs during pairing and synapsis (Penkner et al., 2007; Sato et al., 2009). To test whether SAC proteins also interact with PC-associated proteins to promote synapsis checkpoint signaling, we performed coimmunoprecipitations (co-IPs) of SUN-1::GFP and probed the immunoprecipitates with antibodies

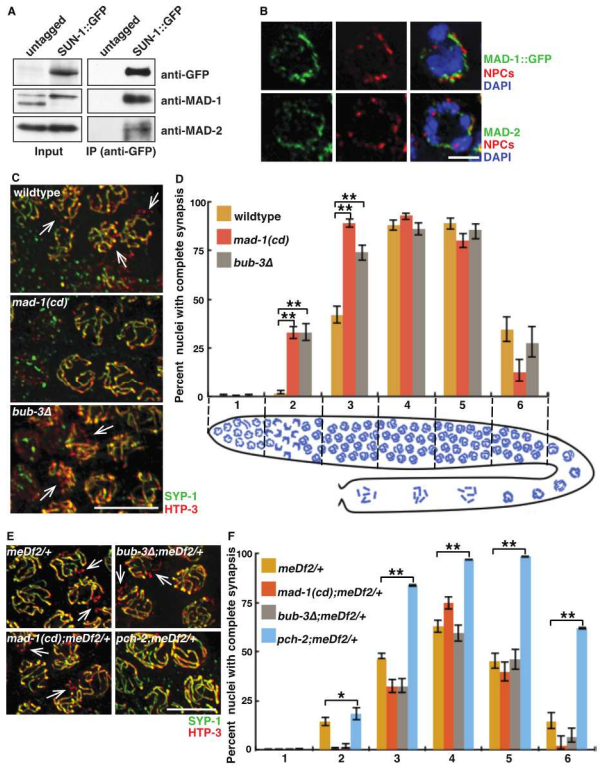

Figure 2-4: SAC proteins interact with PC-associated protein SUN-1, localize to the periphery of meiotic nuclei, and inhibit synapsis in a PC-dependent manner. (A) MAD-1 and MAD-2 coimmunoprecipitate with SUN-1::GFP. Lysates and IPs from untagged and tagged worm strains blotted with antibodies against GFP, MAD-1, and MAD-2. (B) MAD-1::GFP and MAD-2 are at the nuclear periphery marked with NPCs. Images of partial projections of meiotic nuclei stained to visualize DNA (blue), MAD-1::GFP or MAD-2, and NPCs. (C) Images of nuclei during synapsis initiation in wild-type worms and *mad-1(cd)* and *bub-3Δ* mutants stained to visualize SYP-1 and HTP-3. (D) *mad-1(cd)* and *bub-3Δ* mutants accelerate synapsis. Cartoon depicts worm germline. Meiotic progression is from left to right. (E) Mutation of *mad-1* or *bub-3* does not accelerate synapsis in *meDf2/+*. (F) Mutation of *mad-1* or *bub-3* does not rescue the synapsis defect in *meDf2/+*. Images of nuclei in *meDf2/+*, *meDf2/+;mad-1(cd)*, *meDf2/+;bub-3Δ*, and *meDf2/+;pch-2* mutants stained to visualize SYP-1 and HTP-3. (C and F) Arrows indicate unsynapsed chromosomes. Error bars represent 95% confidence intervals. *, P < 0.01; **, P < 0.0001 in all graphs. Bars: (B) 2 µm; (C and F) 5 µm.

against MAD-1 and MAD-2 (Fig. 2-4 A). Both MAD-1 and MAD-2 coimmunoprecipitated with SUN-1::GFP but not with our untagged control (Fig. 2-4 A). We also assessed whether BUB-3 coimmunoprecipitated with SUN-1::GFP but were unable to detect an interaction (not depicted). Therefore, both MAD-1 and MAD-2 interact with the PC-associated protein SUN-1.

We evaluated whether SAC proteins are at the nuclear periphery by staining germlines with antibodies against nuclear pore complexes (NPCs) and MAD-1::GFP or MAD-2. MAD-1::GFP and MAD-2 localized to the nuclear periphery in a punctate pattern (Fig. 2-4 B), and colocalization with SUN-1::GFP confirmed that both proteins were inside the nucleus (not depicted). MAD-1 localization to the nuclear periphery in embryos is dependent on the nonessential NPC component NPP-5 (Ródenas et al., 2012). However, in meiotic nuclei, MAD-1 or MAD-2 localization is not disrupted in *npp-5Δ*, *sun-1Δ*, or *npp-5Δ;sun-1Δ* mutants (not depicted). We stained for BUB-3 but were unable to localize it in meiotic nuclei (not depicted).

We attempted to localize SAC proteins with PCs. However, despite the biochemical interaction with SUN-1, neither MAD-1 nor MAD-2 colocalized with PC proteins in wild-type, *syp-1*, or *meDf2/+* germlines (not depicted). We provide two potential explanations for the inconsistency between our biochemical and cytological experiments: (1) the interaction of SAC proteins at PCs is transient, and/or (2) the pool of MAD-1 and MAD-2 that interacts with PCs is a small fraction of the total protein present in meiotic nuclei. Similar explanations have been made to argue that Mad1 and Mad2 sense tension during mitosis despite an inability to localize these proteins to tensionless kinetochores (Maresca and Salmon, 2010).

MAD-1 and BUB-3 inhibit synapsis in a PC-dependent manner

Given that the synapsis checkpoint component PCH-2 inhibits synapsis (Deshong et al., 2014), we hypothesized that SAC proteins might also regulate this process. We were concerned that defects in germline organization might complicate our analysis (Kitagawa and Rose, 1999; Stein et al., 2007), so we first analyzed meiotic entry in SAC mutants. In *C.*

elegans, premeiotic nuclei undergo mitotic divisions at the distal end of the germline until they enter meiotic prophase (Fig. 2-3 D). Meiotic entry is accompanied by the temporary clustering of chromosomes within nuclei and the appearance of phosphorylated SUN-1 (SUN-1pSer8) at the nuclear envelope (Penkner et al., 2009; Woglar et al., 2013). We assessed whether meiotic entry was affected in SAC mutants by quantifying the number of rows of mitotic germline nuclei from the distal tip to the appearance of SUN-1pSer8 in nuclei with clustered chromosomes (Fig. 2-3 E). Although *mad-2Δ* mutants delayed the onset of meiosis, as indicated by an increased number of rows of mitotic germline nuclei compared with wild-type worms, we did not detect any significant difference in the number of rows of mitotic germline nuclei in wild-type, *mad-1(cd)*, and *bub-3Δ* mutants (Fig. 2-3, E and F). For this reason, additional analysis of meiotic prophase events was performed in *mad-1(cd)* and *bub-3Δ* mutants.

To test whether MAD-1 and BUB-3 negatively regulate synapsis, we assayed SC assembly by staining for HTP-3, an axial element protein that assembles on chromosomes before synapsis (MacQueen et al., 2005), and SYP-1, a central element component whose addition to the SC is concomitant with synapsis (MacQueen et al., 2002). Extensive stretches of HTP-3 without SYP-1 indicate the presence of unsynapsed chromosomes (arrows in Fig. , and colocalization of HTP-3 with SYP-1 indicates complete synapsis (Fig. 2-4 C). Because nuclei in the germline are arrayed in a spatiotemporal gradient, we divided germlines into six equivalent zones and calculated the percentage of nuclei that had completed synapsis (Fig. 2-4 D). *mad-1(cd)* and *bub-3Δ* mutants accelerated synapsis, exhibiting significantly more nuclei with complete synapsis in zones 2 and 3 than wild-type germlines (Fig. 2-4, C and D). Null *mad-1* (*mad-1Δ*) mutants also exhibited normal meiotic entry (Fig. 2-3, E and F) and similar acceleration of synapsis as *bub-3Δ* and *mad-1(cd)* mutants (not depicted). We tested whether accelerated synapsis in *mad-1(cd)* and *bub-3Δ* mutants produced nonhomologous

synapsis by monitoring pairing at a PC locus (HIM-8; Phillips et al., 2005) and a non-PC locus (5S rDNA; Fig. 2-5, C and D). We did not detect any defects in pairing in these mutant backgrounds. These data indicate that MAD-1 and BUB-3 normally restrain synapsis but are not involved in homology assessment.

SAC proteins depend on functional kinetochores to elicit a checkpoint response (Essex et al., 2009). Therefore, we evaluated whether the effect of MAD-1 and BUB-3 on synapsis relied on functional PCs. Because PCs are essential for synapsis, we tested this in *meDf2/+*, in which the loss of a single PC on one of the two X chromosomes

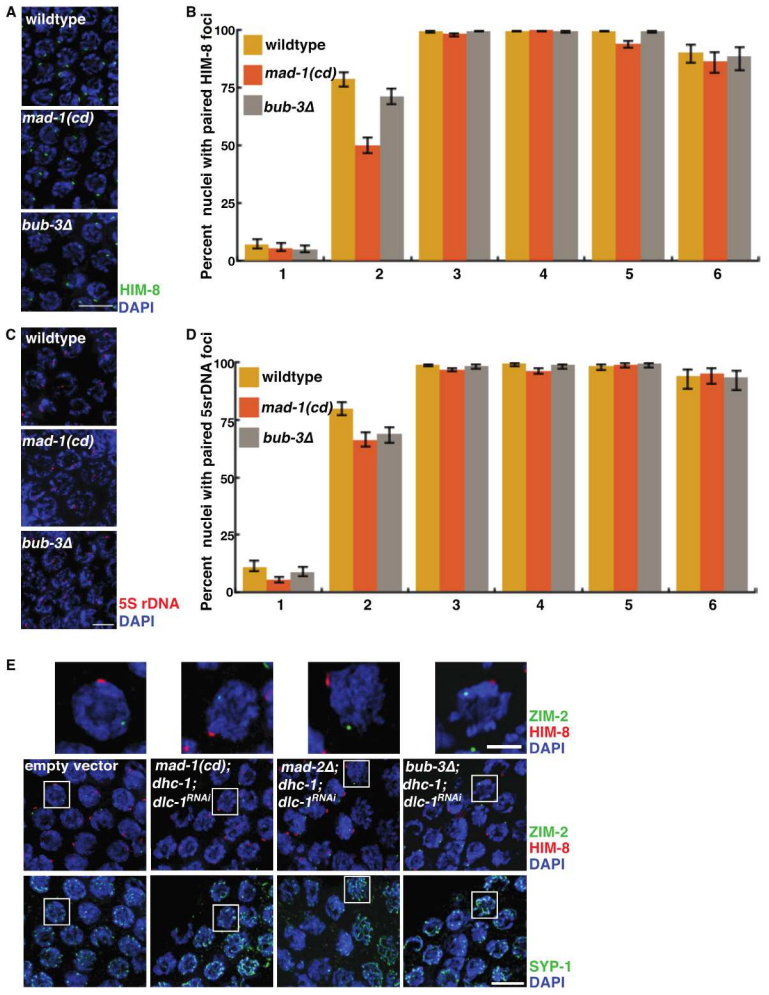

Figure 2-5: Meiotic chromosomes in *mad-1(cd)* and *bub-3Δ* mutants do not undergo nonhomologous synapsis. (A) Images of meiotic nuclei in wild-type worms and *mad-1(cd)and bub-3Δ* mutants stained to visualize DNA (blue) and HIM-8. (B) The X chromosome PC pairs similarly in wild-type worms and in *mad-1(cd) and bub-3Δ* mutants. (C) Images of meiotic nuclei in wild-type worms and *mad-1(cd)* and *bub-3Δ* mutant worms stained to visualize DNA (blue) and the 5S rDNA locus. (D) The 5S rDNA locus pairs similarly in wild-type worms and in *mad-1(cd)* and *bub-3Δ* mutants. (E) Synapsis is homologous in *mad-1(cd);dhc-1;dlc-1^{RNAi}*, *mad-2Δ;dhc-1;dlc-1^{RNAi}*, and *bub-3Δ;dhc-1;dlc-1^{RNAi}* mutants. Images of meiotic nuclei in wild-type, *mad-1(cd);dhc-1;dlc-1^{RNAi}*, *mad-2Δ;dhc-1;dlc-1^{RNAi}*, and *bub-3Δ;dhc-1;dlc-1^{RNAi}* mutant germlines stained to visualize DNA (blue), the autosomal PC protein ZIM-2, and the X chromosome PC protein HIM-8. Also depicted are the same nuclei stained with SYP-1 to verify the presence of synapsed chromosomes. White boxes outline individual fully synapsed nuclei that have paired HIM-8 and ZIM-2 signals. These nuclei are depicted as enlarged images in the top panels. Bars: (A, C, and E [bottom]) 5 µm; (E, top) 2 µm. Error bars represent 95% confidence intervals, whereas *mad-1(cd)*, *mad-1Δ*, *bub-3Δ*, *pch-2;mad-1(cd)*, and *pch-2;bub-3Δ* double mutants do not affect meiotic entry. Bars, 30 µm. Error bars represent ±SEM. *, P < 0.01; **, P < 0.0001

results in a fraction of nuclei exhibiting asynapsis of the X chromosomes (MacQueen et al., 2005). PCH-2's regulation of synapsis does not depend on full PC function because loss of *pch-2* accelerates synapsis even in *meDf2/+*, completely suppressing its synapsis defect (Deshong et al., 2014). Therefore, if MAD-1 or BUB-3's ability to inhibit synapsis depends on PCs, mutation of either of these genes should not affect the rate or extent of synapsis in *meDf2/+*. Unlike *meDf2/+;pch-2* double mutants, *meDf2/+;mad-1(cd)* and *meDf2/+;bub-3Δ* mutants did not accelerate synapsis when compared with *meDf2/+* single mutants (Fig. 2-4 E, zones 2 and 3) and had meiotic nuclei with unsynapsed chromosomes (arrows in Fig. 2-4 F). Therefore, SAC proteins negatively regulate synapsis in a PC-dependent manner.

MAD-1, MAD-2, and BUB-3 enforce the reliance on dynein to promote synapsis

If SAC proteins inhibit synapsis until homologous chromosomes have generated the appropriate amount of dynein-dependent tension, loss of SAC components should abrogate the requirement for dynein in licensing synapsis (Fig. 2-6 B). To test whether mutations in SAC components suppress synapsis defects in dynein mutants, we used a temperature-sensitive mutation of dynein heavy chain, *dhc-1(or195)* (Hamill et al., 2002), which produces defects in both germline mitosis and meiosis. We specifically affected meiotic nuclei by inactivating dynein light chain (*dlc-1*) by RNAi, which partially suppresses the mitotic defects of *dhc-1* mutants (O'Rourke et al., 2007). *dhc-1;dlc-1*^{RNAi} mutants exhibited extensive asynapsis in 95% of germlines, as illustrated by the inability to load SYP-1 onto meiotic chromosomes that have already localized HTP-3 and SYP-1's aggregation into polycomplexes (Fig. 2-6 A; Sato et al., 2009). When we combined *mad-1(cd)*, *mad-1Δ*, *mad-2Δ*, or *bub-3Δ* mutations with *dhc-1;dlc-1*^{RNAi} mutants, we observed robust synapsis (Fig. 2-6 A). We quantified the level of suppression of the asynapsis phenotype and found that 31% of *mad-1(cd);dhc-1;dlc-1*^{RNAi}, 60% of *mad-1Δ;dhc-1;dlc-1*^{RNAi}, 28% of *mad-2Δ;dhc-1;dlc-1*^{RNAi}, and 54% of *bub-3Δ;dhc-1;dlc-1*^{RNAi} germlines exhibited synapsed chromosomes (Fig. 2-6 C).

The synapsis in *mad-1(cd);dhc-1;dlc-1*^{RNAi}, *mad-2Δ;dhc-1;dlc-1*^{RNAi}, and *bub-3Δ;dhc-1;dlc-1*^{RNAi} mutants was homologous, as assayed by staining for the PC proteins ZIM-2 and HIM-8 (Fig. 2-5 E; Phillips et al., 2005; Phillips and Dernburg, 2006). In addition, *mad-1(cd);bub-3Δ;dhc-1;dlc-1*^{RNAi} mutants resembled *bub-3Δ;dhc-1;dlc-1*^{RNAi} mutants with regard to percentage of synapsed germlines (not depicted), indicating that MAD-1 and BUB-3 act in the same pathway. Only 5% of *pch-2;dhc-1;dlc-1*^{RNAi} triple mutants exhibited normal synapsis, similar to *dhc-1;dlc-1*^{RNAi} double mutants (Fig. 2-6 C), suggesting that PCH-2's effect on regulating synapsis is independent of the role that dynein and SAC components play in this process.

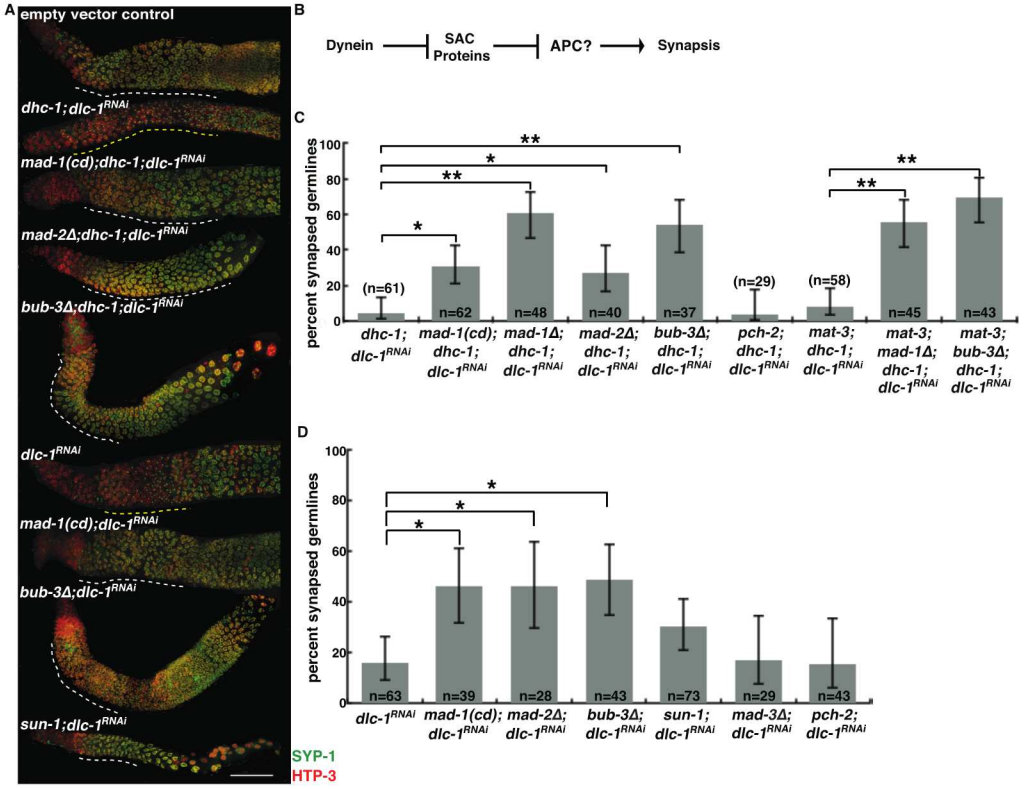

Figure 2-6: Loss of MAD-1, MAD-2, or BUB-3 suppresses the synapsis defects in dynein mutants. (A) Images of germlines from wild-type, *dhc-1;dlc-1*^{RNAi}, *mad-1(cd);dhc-1;dlc-1*^{RNAi}, *mad-2Δ;dhc-1;dlc-1*^{RNAi}, *bub-3Δ;dhc-1;dlc-1*^{RNAi}*;dlc-1*^{RNAi}, *mad-1(cd);dlc-1*^{RNAi}, *mad-2Δ;dlc-1*^{RNAi}, *bub-3Δ;dlc-1*^{RNAi}, and *sun-1;dlc-1*^{RNAi} mutants stained to visualize SYP-1 and HTP-3. Regions of asynapsis are indicated by yellow dashed lines, and regions of normal synapsis are indicated by white dashed lines. Bar, 30 µm. (B) Schematic of the possible role of the APC in regulating synapsis. (C) *mad-1(cd)*, *mad-1Δ*, *mad-2Δ*, or *bub-3Δ* suppresses the synapsis defect in *dhc-1;dlc-1*^{RNAi} germlines. Mutation of *mat-3* does not affect synapsis in *mad-1Δ;dhc-1;dlc-1*^{RNAi} or *bub-3Δ;dhc-1;dlc-1*^{RNAi} mutants. (D) *mad-1(cd)*, *mad-2Δ*, or *bub-3Δ* suppresses the synapsis defect in *dlc-1*^{RNAi} germlines. Error bars represent 95% confidence intervals. *, P < 0.01; **, P < 0.0001.

Similar to a meiosis-specific mutation of *sun-1*, *sun-1(jf18)* (Sato et al., 2009), *mad-1(cd)*, *mad-2Δ*, and *bub-3Δ* mutations suppressed defects in synapsis when only *dlc-1* was knocked down by RNAi (Fig. 2-6, A and D). Loss of *pch-2* also did not suppress the asynapsis phenotype of *dlc-1*^{RNAi} (Fig. 2-6 D). Furthermore, *mad-3Δ;dlc-1*^{RNAi} worms had extensive asynapsis (Fig. 2-6 D), consistent with our finding that *mad-3* is not required for the synapsis checkpoint (Fig. 2-1, B and C).

To further test the involvement of the APC in synapsis (Fig. 2-6 B), we assessed synapsis in *mat-3;dhc-1;dlc-1*^{RNAi} mutants, as well as *mat-3;mad-1Δ;dhc-1;dlc-1*^{RNAi} and *mat-3;bub-3Δ;dhc-1;dlc-1*^{RNAi} mutants. Mutation of *mat-3* had no effect on the percentage of germlines with synapsed chromosomes (Fig. 2-6 C). These data indicate that when specific SAC proteins are absent, the reliance on dynein to license synapsis is lost and this is independent of the APC.

MAD-1 and BUB-3 regulate synapsis by a mechanism redundant with PCH-2

Our experiments in *meDf2/+* (Fig. 2-4, E and F) and dynein mutants (Fig. 2-6, C and D) suggest that SAC components and PCH-2 regulate synapsis by independent mechanisms. If so, loss of both of these mechanisms should affect synapsis more severely than loss of only one. First, we verified that meiotic entry in *pch-2;mad-1(cd)* and *pch-2;bub-3Δ* double mutants was unaffected (Fig. 2-3 F). We then assessed synapsis in *pch-2;mad-1(cd)* and *pch-2;bub-3Δ* double mutants and detected a similar acceleration of synapsis as single mutants, indicating that loss of both of these mechanisms does not further hasten synapsis (Fig. 2-7 A, zones 2 and 3). However, these double mutants, particularly *pch-2;bub-3Δ*, had significantly more nuclei with unsynapsed chromosomes throughout the germline (Fig. 2-7, A [zones 4 and 5] and B). Therefore, loss of both PCH-2 and SAC components produces defects in synapsis that are more severe than any of the single mutants, indicating that the

regulation of synapsis by SAC components and PCH-2 are distinct, biologically parallel processes.

The loss of both SAC components and PCH-2 does not result in nonhomologous synapsis (not depicted), suggesting that the mechanisms controlling synapsis are distinct from those that assess homology between chromosomes. Given that synapsis initiation, not homologous interactions, is the rate-limiting step for synapsis (Rog and Dernburg, 2015) and SC assembly on meiotic chromosomes is highly processive, even when confronted with extensive regions of nonhomologous sequence (MacQueen et al., 2005), it seems likely that synapsis between homologous PCs must overcome multiple barriers, such as those enforced by PCH-2 and SAC components. Why these multiple barriers exist and how they contribute to accurate meiotic chromosome segregation are currently unknown.

We previously proposed that highly stable PC pairing, whether accomplished normally through synapsis or via the inappropriate stabilization of paired PCs, as in *pch-2* mutants,

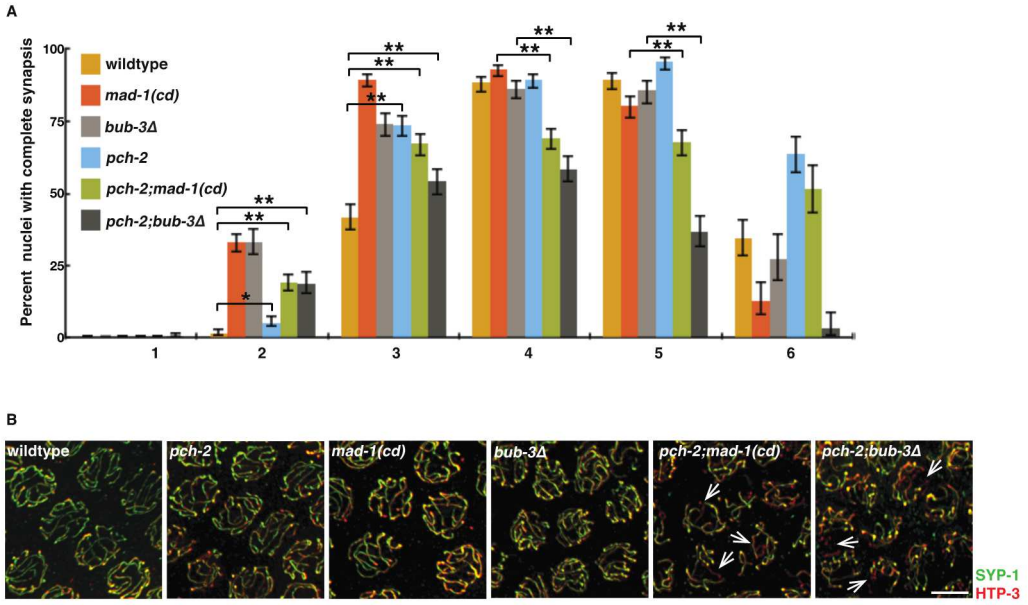

Figure 2-7: Loss of both PCH-2 and MAD-1 or BUB-3 results in more severe defects in synapsis. (A) *pch-2;mad-1(cd)* and *pch-2;bub-3Δ* double mutants exhibit more severe synapsis defects than *pch-2*, *mad-1(cd)*, and *bub-3Δ* single mutants (*mad-1(cd)* and *bub-3Δ* data from 2-4 D). Error bars represent 95% confidence intervals. *, P < 0.01; **, P < 0.0001. (B) Images of nuclei in wild-type worms and *pch-2*, *mad-1(cd)*, *bub-3Δ*, *pch-2;mad-1(cd)*, and *pch-2;bub-3Δ* mutants stained to visualize SYP-1 and HTP-3. Arrows indicate unsynapsed chromosomes. Bar, 5 μm.

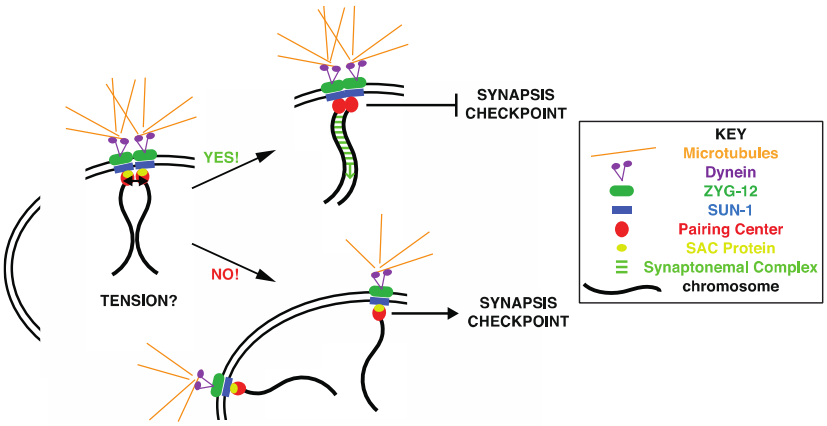

Figure 2-8. M **d checkpoint satisfaction in *C. elegan*** PCs interact with proteins at the nuclear e ZYG-12, to gain access to the cytoplasn l dynein. SAC components are presumed to function at PCs despite our inability to colocalize them. When a chromosome encounters another chromosome, homology is assessed by unknown mechanisms. If chromosomes are homologous and remain stably paired, they resist the pulling forces of the microtubule motor dynein, generating tension (black arrows between PCs) that is monitored by SAC components. Once sufficient tension has been generated (YES!), SAC components are removed, synapsis is initiated, and the checkpoint is silenced. If chromosomes are not homologous, they cannot resist the pulling forces of dynein, are pulled apart, and do not generate tension (NO!). Unsynapsed PCs initiate the synapsis checkpoint response. If unsynapsed chromosomes persist, these nuclei are removed by apoptosis.

satisfies the synapsis checkpoint (Deshong et al., 2014). Our analysis of *mad-1*, *mad-2*, and *bub-3* mutants introduces another layer of complexity to the mechanisms that control synapsis: tension, potentially generated by stably paired PCs, may be translated into a molecular signal that silences the checkpoint and initiates synapsis. Because we cannot cytologically detect SAC components at PCs (not depicted), an alternate interpretation is that SAC components perform some other role at the nuclear envelope that affects the checkpoint and synapsis. However, our data support a model in which once stable PC pairing has generated sufficient tension to resist the pulling forces of the microtubule motor dynein, SAC proteins are either inactivated or removed from PCs to initiate synapsis and the synapsis checkpoint is silenced (Fig. 2-8).

Materials and Methods

Genetics and worm strains

The wild-type *C. elegans* strain background was Bristol N2 (Brenner, 1974). All experiments were performed on adult hermaphrodites at 20°C under standard conditions unless otherwise stated. Mutations and rearrangements used were as follows:

LG I: *mnDp66*, *dhc-1(or195)*, *san-1/mdf-3(ok1580)*, *cep-1(gk138)*

LG II: *fzy-1(h1983)*, *pch-2(tm1458)*, *npp-5(tm3039)*, *bub-3(ok3437)*, *jfSi1[Psun-1::GFP::sun-1::cb-unc-119(+)])*, *mIn1 [mIs14 dpy-10(e128)]*

LG III: *mat-3(or180)*, *jzIs1[pRK139; Ppie-1::GFP::mdf-1::unc-119(+)]*, *unc-119(ed3)*

LG IV: *mdf-2(tm2190)*, *spo-11(ok79)*, *nT1[unc-?(n754) let-?(m435)]*, *nTI [qIs51]*

LG V: *dpy-11(e224)*, *mdf-1(av19)*, *mdf-1(gk2)*, *syp-1(me17)*, *sun-1(jf18)*, *sun-1(ok1282)*, *bcIs39(Pim::ced-1::GFP)*

LG X: *meDf2*.

meDf2 is a terminal deficiency of the left end of the X chromosome that removes the X chromosome PC as well as numerous essential genes (Villeneuve, 1994). For this reason, homo- and hemizygous *meDf2* animals also carry a duplication (*mnDp66*) that includes these essential genes but does not interfere with normal X chromosome segregation (Herman and Kari, 1989) or the synapsis checkpoint (Bhalla and Dernburg, 2005). For clarity, it has been omitted from the text. Because the *mad-2* gene is closely linked to *spo-11*, we used *cep-1* to prevent DNA damage checkpoint–induced apoptosis in *mad2Δ* mutants.

Quantification of germline apoptosis

Scoring of germline apoptosis was performed as previously descried in Bhalla and Dernburg (2005). L4 hermaphrodites were allowed to age for 22 h at 20°C, except for the *mat-3* temperature-sensitive mutation, which was aged for 18 h at the restrictive temperature of 25°C. We verified that MAT-3 function had been reduced by the increase in the number of germline nuclei positive for phosphorylation of histone H3 serine 10 (Golden et al., 2000). Because nuclei progress from mitosis to meiosis as they travel through the germline, this incubation period guaranteed that early meiotic prophase nuclei, but not mitotic nuclei at the start of the germline, had sufficient time to progress to where checkpoint-induced apoptosis occurs in late meiotic prophase (Jaramillo-Lambert et al., 2007). Live worms were mounted under coverslips on 1.5% agarose pads containing 0.2 mM levamisole for wild-type moving strains or 0.1 mM levamisole for *dpy-11* strains. A minimum of 25 germlines were analyzed for each genotype by performing live fluorescence microscopy and counting the number of cells fully surrounded by CED-1::GFP. Significance was assessed using a paired *t* test. All experiments were performed at least twice.

Antibodies, immunostaining, fluorescence in situ hybridization, and microscopy

Immunostaining was performed on worms 20–24 h after L4 stage. Gonad dissections were performed in 1× EBT (250 mM Hepes-Cl, pH 7.4, 1.18 M NaCl, 480 mM KCl, 20 mM EDTA, and 5 mM EGTA) + 0.1% Tween 20 and 20 mM sodium azide. An equal volume of 2% formaldehyde in EBT (final concentration was 1% formaldehyde) was added and allowed to incubate under a coverslip for 5 min. The sample was mounted on HistoBond slides (75 × 25 × 1 mm from Lamb), freeze-cracked, and incubated in methanol at −20°C for slightly more than 1 min and transferred to PBST (PBS with Tween 20). After several washes of PBST, the samples were incubated for 30 min in 1% bovine serum albumin diluted in PBST. A hand-cut paraffin square was used to cover the tissue with 50 µl of antibody solution. Incubation was

conducted in a humid chamber overnight at 4°C. Slides were rinsed in PBST and then incubated for 2 h at room temperature with fluorophore-conjugated secondary antibody at a dilution of 1:500. Samples were rinsed several times and DAPI stained in PBST, then mounted in 13 µl of mounting media (20 M *N*-propyl gallate [Sigma-Aldrich] and 0.14 M Tris in glycerol) with a no. 1 1/2 (22 mm^2) coverslip, and sealed with nail polish.

Primary antibodies were as follows (dilutions are indicated in parentheses): rabbit anti–SYP-1 (1:500; MacQueen et al., 2002), chicken anti–HTP-3 (1:250; MacQueen et al., 2005), rabbit anti–MAD-2 (1:10,000; Essex et al., 2009), mouse anti-NPC MAb414 (1:5,000; Covance; Davis and Blobel, 1986), guinea pig anti–HIM-8 (1:250; Phillips et al., 2005), rat anti–HIM-8, guinea pig anti–ZIM-2 (1:2,500; Phillips and Dernburg, 2006), guinea pig anti–SUN-1pSer8 (1:500; Penkner et al., 2009), and goat anti-GFP (1:10,000; Hua et al., 2009). Secondary antibodies were Cy3 anti–mouse, anti–rabbit, anti–guinea pig, anti–rat, and anti–chicken (Jackson ImmunoResearch Laboratories, Inc.) and Alexa Fluor 488 anti–goat, anti–guinea pig, and anti–rabbit (Invitrogen). Antibodies against SYP-1 were provided by A. Villeneuve (Stanford University, Palo Alto, CA). Antibodies against HTP-3, HIM-8, and ZIM-2 were provided by A. Dernburg (University of California, Berkeley/E.O. Lawrence Berkeley National Lab, Berkeley, CA). Antibodies against MAD-2 were provided by A. Desai (Ludwig Institute/University of California, San Diego, La Jolla, CA). Antibodies against SUN-1pSer8 were provided by V. Jantsch (Max F. Perutz Laboratories, Vienna, Austria). Antibodies against GFP were provided by S. Strome (University of California, Santa Cruz, Santa Cruz, CA).

Fluorescence in situ hybridization was performed as described in Phillips et al. (2005). 5S rDNA probe was generated using genomic DNA as a template by PCR and gel purified. The PCR product was digested with the TasI restriction enzyme and ethanol precipitated. 10 µg of digested DNA was diluted into 50 µl water, denatured for 2 min at 95°C, chilled on ice, and

spun briefly. At room temperature, 20 µl Roche 5× TdT reaction buffer (Tris-HCl, pH 7.2, potassium cacodylate, and BSA), 20 µl of 25 mM $CoCl_2$ solution, 3.3 ml of 1 mM aa-dUTP, 6.6 ml of 1 mM unlabelled dTTP, and 2 µl (800 U) recombinant terminal deoxynucleotidyl transferase were added. This solution was incubated for 1 h at 37°C. EDTA was added to 5 mM, and the DNA was ethanol precipitated. The probe was conjugated with Cy3 dye (Life Technologies) by adding 5 µl of 1 mg/ml resuspended probe and 3 µl of 1 M bicarbonate buffer to one aliquot of dry dye. The reaction was mixed, shielded from light, and incubated for 1 h at room temperature and ethanol precipitated.

Worms were dissected 24 h after L4 stage in 30 µl EBT (1× egg buffer, 0.1% Tween 20, and 20 mM sodium azide). We added 30 µl of 1× egg buffer and 0.5% EGS (ethylene glycol bis[succinimidylsuccinate] in dimethyl formamide) and pipetted to extrude gonads. 30 µl of this liquid was removed, and the sample was mounted on HistoBond slides (75 × 25 × 1 mm from Lamb) and allowed to incubate in a humid chamber for 30 min at room temperature. Samples were freeze-cracked and incubated in methanol at −20°C for slightly more than 1 min and transferred to 2× SSCT (2× SSC and 0.1× Tween 20) at room temperature. Samples were placed in 3.7% formaldehyde in 1× egg buffer for 5 min, rinsed briefly in 2× SSCT, and washed twice in 2× SSCT for 5 min. The samples were incubated in 50% formamide in 2× SCCT for 5 min, transferred to fresh 50% formamide in 2× SCCT, and incubated at 37°C overnight. Samples were cooled to room temperature, and 20 ng of 5S rDNA probe in hybridization solution (50% formamide, 3% SSC, 10% dextran sulphate) was added and sealed onto the sample with a coverslip and nail polish. Slides were denatured on a hot block at 95°C for 3 min and placed in a humid chamber at 37°C overnight. Coverslips were removed, and the samples were washed twice in 50% formamide in 2× SSCT for 30 min each. Samples were rinsed several times and DAPI stained in 2× SSCT. Samples were mounted in 13 µl of mounting media (20 M *N*-propyl gallate [Sigma-Aldrich] and 0.14 M Tris in glycerol) with a no. 1 1/2 (22 mm^2) coverslip and sealed with nail polish.

Quantification of synapsis and pairing was performed with a minimum of three whole germlines per genotype as in Phillips et al. (2005) on animals 24 h after L4 stage. The gonads were divided into six equal-sized regions, beginning at the distal tip of the gonad and progressing through the end of pachytene. Significance was assessed by performing Fisher's exact test.

Quantification of rows of mitotic nuclei was performed as in Stevens et al. (2013), and a minimum of 18 germlines were analyzed on animals 24 h after L4 stage. Significance was assessed by performing a paired *t* test.

Quantification of meiotic progression was performed with a minimum of three whole germlines per genotype on animals 24 h after L4 stage by quantifying the percentage of nuclei with clustered chromosomes. Significance was assessed by performing Fisher's exact test.

All images were acquired at room temperature using a DeltaVision Personal DV system (GE Healthcare) equipped with a 100× NA 1.40 oil immersion objective (Olympus), resulting in an effective xy pixel spacing of 0.064 or 0.040 µm. Images were captured using a charge-coupled device camera (Cool-SNAP HQ; Photometrics). Three-dimensional image stacks were collected at 0.2-µm z-spacing and processed by constrained, iterative deconvolution. Imaging, image scaling, and analysis were performed using functions in the softWoRx software package. Projections were calculated by a maximum intensity algorithm. Composite images were assembled, and some false coloring was performed with Photoshop software (Adobe).

IPs

Asynchronous liquid worm cultures were grown at 20°C for 4 d in S medium supplemented with concentrated HB101 bacteria, and embryos were extracted in a sodium hypochlorite

solution (25% [vol/vol] NaClO and 0.25% [vol/vol] 10N NaOH) and allowed to hatch overnight on unseeded NGM plates. Hatched L1s were washed off NGM plates and grown at 19°C for 66–68 h or until the majority of animals reached adulthood. Adult worms were harvested, washed twice in sterile water and once in buffer H0.15 (50 mM Hepes, pH 8.0, 2 mM $MgCl_2$, 0.1 mM EDTA, pH 8.0, 0.5 mM EGTA-KOH, pH 8.0, 15% glycerol, 0.1% NP-40, and 150 mM KCl), and frozen into "popcorn" by dripping into liquid nitrogen. Popcorn was then pulverized three times for 2 min at 25 Hz in a MM-400 mixer mill (Retsch Technology) with liquid nitrogen immersion between milling sessions. Worms were lysed by adding 5 ml ice-cold buffer H0.15 supplemented with protease and phosphatase inhibitors (0.1 mM AEBSF, 5 mM benzamidine, 1:200 aprotinin, Roche Complete Mini tablets w/o EGTA, 1 mM $Na_4P_2O_7$, 2 mM Na-β-glycerophosphate, 0.1 mM Na_3VO_4, and 5 mM NaF) to 2 g of worm powder. Lysis was continued by rotating at 4°C, followed by sonicating twice for 30 s at 40% amplitude on ice (Braun). Lysate was then spun at 48,000 *g* for 20 min at 4°C in a JA-20 rotor (Beckman Coulter). IPs were performed as in Akiyoshi et al. (2009) with 50 µl protein G Dynabeads (Invitrogen) cross-linked to 12.5 µg mouse GFP antibody (Roche).

For immunoblotting, samples were run on SDS-PAGE gels, transferred to nitrocellulose, blocked in a PBST + 5% (wt/vol) nonfat milk solution, and then probed with mouse anti-GFP (1:1,000; Roche), rabbit anti–MAD-1 (1:2,000; Yamamoto et al., 2008), or rabbit anti–MAD-2 (1:5,000; Essex et al., 2009) overnight at 4°C. Blots were washed three times for 10 min in PBST, probed for 1 h using an HRP-conjugated secondary antibody (rabbit or mouse; GE Healthcare), washed three times for 10 min in PBST, and then analyzed using a chemiluminescent substrate (Thermo Fisher Scientific). 0.1% of starting material is shown for all input samples, 10% of the IP elution is shown for anti-GFP Western blots, and 30% of IPs are shown for anti–MAD-1 and anti–MAD-2 Western blots. IP samples were analyzed with Pico chemiluminescent substrate (Thermo Fisher Scientific), and input samples were

analyzed using Dura enhanced chemiluminescent substrate (Thermo Fisher Scientific). We estimate IP to have purified between 20 and 30% of SUN-1::GFP present in the input.

Feeding RNAi

For RNAi, *dlc-1*^{RNAi} and empty vector (L4440) clones from the Ahringer laboratory (Fraser et al., 2000) were used. Bacteria strains containing *dlc-1*^{RNAi} and empty vector controls were cultured overnight in 10 ml Luria broth + 50 µg/µl carbenicillin, centrifuged, and resuspended in 0.5 ml Luria broth + 50 µg/µl carbenicillin. 60 µl of the RNAi bacteria was spotted onto NGM plates containing 1 mM IPTG + 50 µg/µl carbenicillin and allowed to grow at room temperature overnight. L4 hermaphrodite worms were picked into M9, transferred to these plates, allowed to incubate for 2–3 h, and then transferred to fresh RNAi plates to be dissected 48 h after L4. Strains with the *dhc-1* temperature-sensitive mutation were rinsed in M9, plated on *dlc-1*^{RNAi} plates, incubated at 15°C for 24 h, and then shifted to the restrictive temperature of 25°C for 24 h and dissected 48 h after L4 as previously described (Sato et al., 2009). A minimum of 28 germlines were scored for each genotype. Significance was assessed by performing Fisher's exact test.

Chapter 3: Synaptonemal complex components are required for meiotic checkpoint function in *C. elegans*

Introduction

Meiosis is the specialized cell division by which cells undergo one round of DNA duplication and two successive rounds of division to produce haploid gametes from diploid organisms. During sexual reproduction, fertilization restores diploidy to the resulting embryo. In order for meiotic chromosomes to segregate properly in meiosis I and II, homologs pair, synapse and undergo crossover recombination (Bhalla et al., 2008). If homologous chromosomes fail to segregate properly, this can produce gametes, such as egg and sperm, with an improper number of chromosomes, termed aneuploidy. Embryos that result from fertilization of aneuploid gametes are generally inviable, but can also exhibit developmental disorders (Hassold and Hunt, 2001). Therefore, checkpoint mechanisms monitor early meiotic prophase events to avoid the production of aneuploid gametes (MacQueen and Hochwagen, 2011).

Synapsis involves the assembly of a proteinaceous complex, the synaptonemal complex (SC), between paired homologous chromosomes and is essential for crossover recombination (Bhalla and Dernburg, 2008). In *C. elegans*, the synapsis checkpoint induces apoptosis to remove nuclei with unsynapsed chromosomes and prevent aneuploid gametes (Bhalla and Dernburg, 2005) (Fig. 3-1 A). The synapsis checkpoint requires Pairing Centers (PCs) (Bhalla and Dernburg, 2005), *cis*-acting sites near one end of each chromosome. PCs also promote pairing and synapsis (MacQueen et al., 2005) by recruiting factors, such as the zinc-finger containing proteins ZIM-1, ZIM-2, ZIM-3 and HIM-8 (Phillips et al., 2005) (Phillips and Dernburg, 2006), and the conserved polo-like kinase PLK-2 (Harper et al., 2011) (Labella et al., 2011). We have hypothesized that the synapsis checkpoint monitors the stability of pairing at PCs as a proxy for proper synapsis (Deshong et al., 2014) (Bohr et al., 2015). However, whether the process of synapsis is also monitored by the synapsis checkpoint is currently unknown.

Upon entry into meiosis, axial elements assemble between replicated sister chromatids to support homolog pairing and synapsis. In most species, axial elements consist of HORMA domain proteins (HORMADs) (Hollingsworth et al., 1990) (Aravind and Koonin, 1998) (Caryl et al., 2000) (Fukuda et al., 2010) (Wojtasz et al., 2009). In *C. elegans*, four HORMAD proteins, HTP-3, HIM-3, HTP-1, and HTP-2, comprise the axial elements of the SC and play overlapping but distinct roles during meiotic prophase (Zetka et al., 1999) (Couteau et al., 2004) (Couteau and Zetka, 2005) (Martinez-Perez and Villeneuve, 2005) (Goodyer et al., 2008). Synapsis is complete when the central element of the SC is assembled between paired axial elements of homologous chromosomes. In *C. elegans*, the central element includes the factors SYP-1, SYP-2, SYP-3 and SYP-4 (MacQueen et al., 2002) (Colaiacovo et al., 2003) (Smolikov et al., 2007) (Smolikov et al., 2009). Loss of any one of these proteins produces a similar mutant phenotype: extensive asynapsis of all chromosomes and a delay in meiotic progression (MacQueen et al., 2002) (Colaiacovo et al., 2003) (Smolikov et al., 2007) (Smolikov et al., 2009). In *syp-1* mutants, the synapsis checkpoint response induces germline apoptosis (Fig. 3-1 A) (Bhalla and Dernburg, 2005). However, it's unclear whether *syp-2*, *syp-3* or *syp-4* mutants elicit the same checkpoint response as *syp-1* mutants. Genetically ablating the checkpoint response does not affect the meiotic delay associated with asynapsis in *syp-1* mutants (Deshong et al., 2014) (Bohr et al., 2015), indicating that these two events are not mechanistically coupled. Recent work has implicated the HORMADs as a primary mediator of this delay (Kim et al., 2015).

Here, we report that some SC components are required for the synapsis checkpoint. *syp-2* mutants resemble *syp-1* mutants and elevate apoptosis in response to the synapsis checkpoint. *syp-4* mutants also exhibit elevated apoptosis similar to *syp-1* and *syp-2* mutants. However, the elevation in apoptosis observed in *syp-4* mutants is not dependent on the synapsis checkpoint component PCH-2, suggesting there may be differences in the way the synapsis checkpoint can be regulated. By contrast, *syp-3* mutants do not elicit a synapsis checkpoint response, showing that SYP-3 is required for the synapsis checkpoint. Similarly,

htp-3, *him-3* and *htp-1* mutants are also defective in the synapsis checkpoint. Finally, loss of SYP-3, HTP-3, HIM-3 or HTP-1 does not abrogate PC function, consistent with these proteins playing a direct role in the checkpoint.

Results and Discussion

SYP-3 is required for the synapsis checkpoint

syp-1 mutants exhibit increased germline apoptosis as a result of the synapsis checkpoint (due to asynapsis) and the DNA damage checkpoint (due to an inability to repair double strand breaks [DSBs]) (Fig. 3-1 A) (Bhalla and Dernburg, 2005). SPO-11 is required for the introduction of meiotic DSBs (Dernburg et al., 1998) and PCH-2 is required for the synapsis checkpoint (Bhalla and Dernburg, 2005). We've previously shown that loss of SPO-11 or PCH-2 in otherwise wild-type backgrounds does not affect germline apoptosis (Bhalla and Dernburg, 2005). However, *syp-1;spo-11* and *pch-2;syp-1* double mutants display lower levels of germline apoptosis than *syp-1* single mutants because of loss of the DNA damage or synapsis checkpoint response, respectively. (Fig. 3-1 A) (Bhalla and Dernburg, 2005). Loss of both checkpoints in *pch-2;spo-11;syp-1* triple mutants result in wild-type levels of apoptosis (Fig. 3-1 A) (Bhalla and Dernburg, 2005).

To determine if other *syp* mutants behave similarly we quantified apoptosis in null *syp-2*, *syp-3* and *syp-4* mutants (Fig. 3-1, B, C and D). Mutation of *syp-2* elevated germline apoptosis levels similar to those seen in *syp-1* mutants (Fig. 3-1 B), suggesting that *syp-2* mutants exhibit both DNA damage and synapsis checkpoint responses. To verify that *syp-2* mutants exhibit a DNA damage checkpoint response, we introduced a mutation of *spo-11* into a *syp-2* background. We observed decreased apoptosis to intermediate levels in *syp-2;spo-11* double mutants (Fig. 3-1 B), indicating that *syp-2* mutants exhibit a DNA damage checkpoint response. To determine if *syp-2* mutants exhibit a synapsis checkpoint response we observed apoptosis in *syp-2;pch-2* double mutants which also had intermediate levels of germline apoptosis (Fig. 3-1 B). This verifies that *syp-2* mutants elevate germline apoptosis

due to the synapsis checkpoint. Furthermore, mutation of both *pch-2* and *spo-11* reduced apoptosis to wild-type levels in a *syp-2* background (Fig. 3-1 B). These data indicate that the elevation of apoptosis observed in *syp-2* mutants is in response to both the DNA damage and synapsis checkpoints, similar to *syp-1* mutants (Bhalla and Dernburg, 2005).

Next we analyzed *syp-4* mutants and found that germline apoptosis was also elevated (Fig. 3-1 C) comparable to *syp-1* and *syp-2* mutants (Fig. 3-1 B). Moreover, *spo-11;syp-4* double mutants resembled *spo-11;syp-1* and *spo-11;syp-2* double mutants (Fig. 3-1, B and C), (Bhalla and Dernburg, 2005) indicating that *syp-4* mutants have elevated apoptosis due to the DNA damage checkpoint. However, germline apoptosis was unaffected in *syp-4;pch-2*

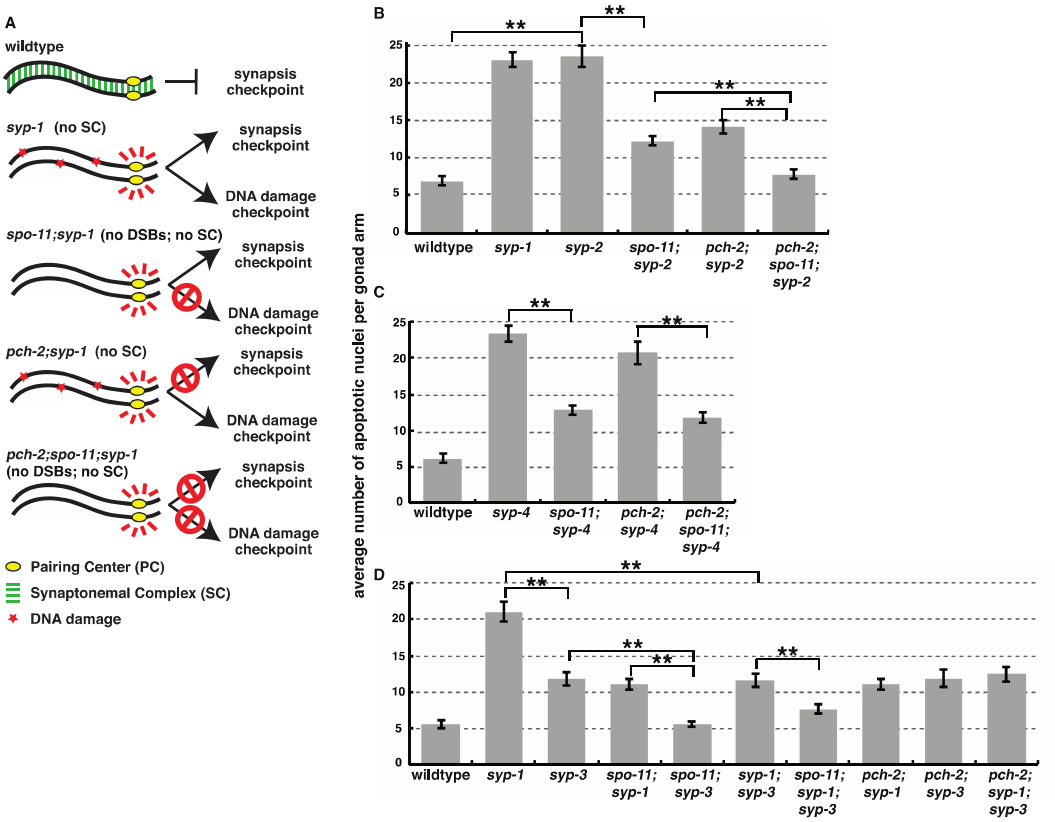

Figure 3-1: MAD-1, MAD-2, and BUB-3 are required for the synapsis checkpoint. SYP-3 is required for the meiotic synapsis checkpoint. (A) Cartoons depicting meiotic checkpoint activation in *C. elegans*. (B) Elevation of germline apoptosis in *syp-2* mutants is dependent on *spo-11* and *pch-2*. (C) Elevation of germline apoptosis in *syp-4* mutants is dependent on *spo-11* but not on *pch-2*. (D) Elevation of germline apoptosis in *syp-3* mutants is dependent on *spo-11* but not on *pch-2*. Mutation of *syp-3* reduces apoptosis in *syp-1* and *syp-1;spo-11* double mutants but not *syp-1;pch-2* double mutants. Error bars represent ±SEM. A * indicates a p value < 0.01 and a ** indicates a p value < 0.0001.

and *syp-4;pch-2;spo-11* mutants compared to *syp-4* and *syp-4;spo-11* mutants, respectively

(Fig. 3-1 C). From these data we conclude that there is either another unknown meiotic checkpoint that leads to elevated apoptosis in *syp-4* mutants or that the genetic requirements for the synapsis checkpoint in *syp-4* mutants are different than that of *syp-1* and *syp-2* mutants.

We also quantified apoptosis in *syp-3* mutants and observed increased apoptosis compared to wild-type worms but not to levels observed in *syp-1* single mutants (Fig. 3-1 D). This suggests that unlike *syp-1, syp-2 and syp-4* mutants, *syp-3* mutants either have a functional DNA damage or synapsis checkpoint, but not both. To determine which checkpoint was responsible for the elevated apoptosis observed in *syp-3* mutants we first quantified apoptosis in *syp-3;spo-11* double mutants (Fig. 3-1 D). Mutation of *spo-11* in a *syp-3* background reduced apoptosis to wild-type levels (Fig. 3-1 D), indicating that the elevation in apoptosis observed in *syp-3* mutants is dependent on the DNA damage checkpoint. To ensure that the elevation in apoptosis observed in *syp-3* mutants is due solely to the DNA damage checkpoint and not due to the synapsis checkpoint, we monitored germline apoptosis in *syp-3;pch-2* mutants. Mutation of *pch-2* in the *syp-3* background did not reduce apoptosis (Fig. 3-1 D), indicating that the elevation in apoptosis observed in *syp-3* mutants is not dependent on the synapsis checkpoint. Therefore, although chromosomes are unsynapsed in *syp-3* mutants (Smolikov et al., 2007), the synapsis checkpoint response is abrogated.

These data suggest that SYP-3 is required for the synapsis checkpoint. To verify this, we quantified apoptosis in *syp-3;syp-1* double mutants (Fig. 3-1 D). *syp-3;syp-1* double mutants had intermediate levels of germline apoptosis (Fig. 3-1 D), indicating loss of either the DNA damage checkpoint or the synapsis checkpoint but not both. Mutation of *syp-3* in a *pch-2;syp-1* background did not further decrease apoptosis (Fig. 3-1 D), confirming that SYP-3 is not required for the DNA damage checkpoint. However, *syp-3;spo-11;syp-1* triple mutants had wild-type levels of apoptosis (Fig. 3-1 D), signifying loss of the synapsis checkpoint. Altogether these data show that SYP-3, but not SYP-2 or SYP-4, is required for the synapsis

checkpoint.

HORMAD proteins HTP-3, HIM-3 and HTP-1 are required for the synapsis checkpoint

Imaging of meiotic chromosomes by electron microscopy in *C. elegans* suggests that SYP-3 is closely associated with the axial elements of the SC (Schild-Prufert et al., 2011). Because of this, we decided to test whether axial element proteins, specifically HORMADs, are required for the synapsis checkpoint using null mutations of each gene (Fig. 3-2). First, we tested whether HTP-3 and HIM-3 are required for the synapsis checkpoint by monitoring apoptosis in *htp-3* and *him-3* mutants (Fig. 3-2 A). *htp-3* and *him-3* mutants produced wild-type levels of apoptosis (Fig. 3-2 A), despite their inability to synapse chromosomes (Goodyer et al., 2008) (Zetka et al., 1999). Thus, these mutants elicit neither a DNA damage checkpoint nor a synapsis checkpoint response. HTP-3 is required for DSB formation in meiosis (Goodyer et al., 2008) and HIM-3 is thought to promote inter-homolog recombination by inhibiting inter-sister repair (Couteau and Zetka, 2011) (Couteau et al., 2004) (Martinez-Perez et al., 2008). These phenotypes could explain the inability of these mutants to generate a DNA damage response. To further investigate a possible role for HTP-3 and HIM-3 in the synapsis checkpoint, we introduced mutations of *htp-3* and *him-3* into *syp-1* mutants and quantified apoptosis. *htp-3;syp-1* and *him-3;syp-1* double mutants have wild-type levels of germline apoptosis (Fig. 3-2 A), indicating that, even in the *syp-1* background, HTP-3 and HIM-3 are indeed required for the synapsis checkpoint.

We then tested whether HTP-1 and HTP-2 are required for the synapsis checkpoint. *htp-1* single mutants synapse their chromosomes non-homologously (Couteau and Zetka, 2005) (Martinez-Perez and Villeneuve, 2005) and had intermediate levels of apoptosis (Fig. 3-2B).

These data suggest that *htp-1* mutants elicit a DNA damage or synapsis checkpoint response but not both. *htp-2* single mutants have no obvious meiotic defects (Couteau and Zetka, 2005) and exhibited wild-type levels of apoptosis (Fig. 3-2 B), indicating that *htp-2* mutants do not produce a DNA damage or synapsis checkpoint response. *htp-1* is close to *spo-11* on chromosome IV, making it difficult to create *htp-1 spo-11* double mutants. Therefore, to investigate which checkpoint was responsible for the intermediate levels of apoptosis observed in *htp-1* mutants we instead abrogated the DNA damage checkpoint using a mutation in *cep-1*, the *C. elegans p53* orthologue (Derry et al., 2001) (Schumacher et al., 2001).

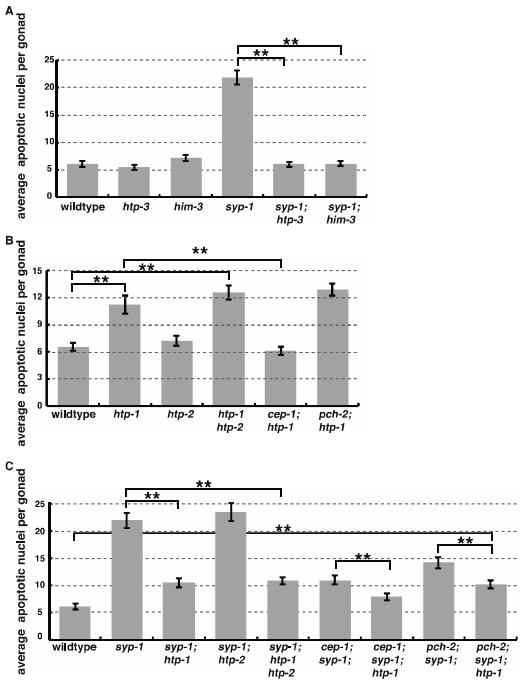

Figure 3-2: HTP-3, HIM-3 and HTP-1 are required for the synapsis checkpoint. (A) *htp-3 and him-3* mutants have wild-type levels of germline apoptosis and reduce germline apoptosis in *syp-1* mutants. (B) The elevation of germline apoptosis in *htp-1* mutants is *cep-1* dependent but not *pch-2* dependent. (C) Mutation of *htp*-1 reduces germline apoptosis in *syp-1* single and *cep-1;syp-1* double mutants. . Error bars represent ±SEM. A * indicates a p value < 0.01 and a ** indicates a p value < 0.0001.

Mutation of *cep-1* in the *htp-1* background reduced apoptosis to wild-type levels while mutations of *pch-2* had no effect on germline apoptosis when compared to *htp-1* single mutants (Fig. 3-2 B). This indicates that the elevation in apoptosis observed in *htp-1* mutants is dependent on the DNA damage checkpoint and not the synapsis checkpoint. Furthermore, these data suggest that either non-homologous synapsis does not result in a synapsis checkpoint response or that HTP-1 may be required for the synapsis checkpoint.

To test if HTP-1 is required for the synapsis checkpoint, we took advantage of the partially redundant roles of HTP-1 and HTP-2 during meiotic synapsis. *htp-1 htp-2* double mutants have unsynapsed chromosomes (Couteau and Zetka, 2005) (Martinez-Perez and Villeneuve, 2005), similar to *htp-3* and *him-3* single mutants (Goodyer et al., 2008) (Zetka et

al., 1999), allowing us to evaluate whether unsynapsed chromosomes elicit a synapsis checkpoint response in the absence of HTP-1. Similar to *htp-1* single mutants, *htp-1 htp-2* double mutants exhibited intermediate apoptosis (Fig. 3-2 B), showing that abrogation of the synapsis checkpoint in *htp-1* mutants is not the product of non-homologous synapsis and supporting the possibility that HTP-1 is required for the synapsis checkpoint. Moreover, unlike *htp-3* and *him-3* mutants (Figure 3-2 A), *htp-1* and *htp-2* single mutants, as well as *htp-1 htp-2* double mutants, activate germline apoptosis in response to the DNA damage checkpoint (Fig. 3-2 B), further supporting the idea that meiotic HORMADS also play distinct roles during meiotic prophase. In addition, these data demonstrate that HTP-1 and HTP-2 do not appear to play redundant roles in the DNA damage checkpoint's induction of germline apoptosis. This is in contrast to the redundant roles they play in regulating meiotic progression when chromosomes are unsynapsed (Kim et al., 2015).

To further validate that HTP-1 is required for the synapsis checkpoint we observed apoptosis in *htp-1;syp-1* and *htp-2;syp-1* double mutants (Fig. 3-2 C). While mutation in *htp-2* had no effect on apoptosis in the *syp-1* background, we observed reduced apoptosis to intermediate levels in *htp-1;syp-1* double mutants compared to *syp-1* single mutants (Fig. 3-2 C), indicating loss of one checkpoint. To verify that the synapsis checkpoint but not the DNA damage checkpoint is abrogated in the *htp-1*;*syp-1* background we observed apoptosis in *htp-1;pch-2*;*syp-1 and htp-1;cep-1;syp-1* triple mutants. Mutation of *cep-1* in the *htp-1;syp-1* background reduced apoptosis to levels comparable to wild-type worms (Fig. 3-2 C) demonstrating that the elevation of apoptosis observed in *htp-1;syp-1* mutants is dependent on the DNA damage checkpoint. In addition, mutation of *pch-2* did not further decrease apoptosis in the *htp-1;syp-1* background (Fig. 3-2 C), showing that the elevation of apoptosis observed in *htp-1;syp-1* mutants is not dependent on the synapsis checkpoint. Therefore, the synapsis checkpoint is abrogated in *htp-1;syp-1* mutants. However, while apoptosis in *htp-1;pch-2*;*syp-1* triple mutants was significantly higher than wildtype, *htp-1;pch-2*;*syp-1* triple mutants had reduced levels of apoptosis in comparison to *pch-2;syp-1* double mutants (Fig.

3-2 C), suggesting that loss of HTP-1 affects the synapsis checkpoint more severely than loss of PCH-2. Lastly, similar to *htp-1;syp-1* double mutants, *htp-1 htp-2;syp-1* triple mutants exhibited intermediate levels of apoptosis compared to *syp-1* single mutants and wild-type worms (Fig. 3-2 C), further verifying that HTP-2 is not redundant with HTP-1 when considering checkpoint activation of apoptosis. Altogether, these data show that HTP-3, HIM-3, and HTP-1, but not HTP-2, are required for the synapsis checkpoint.

HTP-3 and HIM-3 disrupt localization of some but not all PC proteins

HTP-3, HIM-3 and HTP-1 could be directly required for the synapsis checkpoint or these proteins could be involved in regulating other mechanisms that are required for the synapsis checkpoint. For example, since PCs are required for the synapsis checkpoint (Bhalla and Dernburg, 2005), we were concerned that *htp-3, him-3* and *htp-1* mutants might have defects in PC function. Since *htp-1* single mutants produce non-homologous synapsis (Couteau and Zetka, 2005) (Martinez-Perez and Villeneuve, 2005) and our analysis of apoptosis indicates that loss of HTP-2 has no effect on synapsis checkpoint signaling (Fig. 3-2 C), we performed experiments to address this using *htp-1 htp-2* double mutants, which have unsynapsed chromosomes (Couteau and Zetka, 2005) (Martinez-Perez and Villeneuve, 2005) allowing better comparison with *htp-3* and *him-3* single mutants. We localized ZIM-2, a protein that binds to and is required for PC function of Chromosome V (Phillips and Dernburg, 2006), in wild-type worms and *htp-3*, *him-3* and *htp-1 htp-2* mutants in early meiotic prophase nuclei (Fig. 3-3 A). In wild-type worms ZIM-2 forms robust patches at the nuclear periphery in these nuclei (Fig. 3-3 A) (Phillips and Dernburg, 2006). We observed ZIM-2 staining in *htp-1 htp-2* double mutants similar to wild-type worms (Fig. 3-3 A). However, *htp-3* and *him-3* mutants had less robust ZIM-2 localization compared to wild-type worms (Fig. 3-3 A). We saw similar results in *htp-3*, *him-3* and *htp-1 htp-2* mutants when we stained for ZIM-1 and ZIM-3 (data

not shown), which bind the PCs of Chromosomes I and IV and Chromosomes II and III, respectively (Phillips and Dernburg, 2006).

The defect in robustly localizing ZIMs to PCs in *htp-3* and *him-3* mutants (Fig. 3-3 A) might explain why these mutants are defective in the synapsis checkpoint. However, a single unsynapsed X chromosome, with an active PC, is sufficient to elicit a checkpoint response (Bhalla and Dernburg, 2005). Therefore, we also localized the X chromosome PC binding protein, HIM-8 (Figure 3C) (Phillips et al., 2005). We observed staining patterns similar to wild-type worms in *htp-3*, *him-3* and *htp-1 htp-2* mutants (Fig. 3-3 B). We also determined whether X chromosome PCs were functional in these mutant backgrounds by localizing PLK-2 (Fig. 3-3 B), a kinase that is recruited by PCs to promote synapsis and the synapsis checkpoint (Harper et al., 2011) (Labella et al., 2011). In *htp-3*, *him-3* and *htp-1 htp-2* mutants, PLK-2 co-localized with HIM-8 (Fig. 3-3 B), indicating X chromosome PCs were active. Altogether, these data argue against the interpretation that mutations in HORMAD proteins abrogate the synapsis checkpoint indirectly due to defects in PC function and support the conclusion that they are involved in the synapsis checkpoint response.

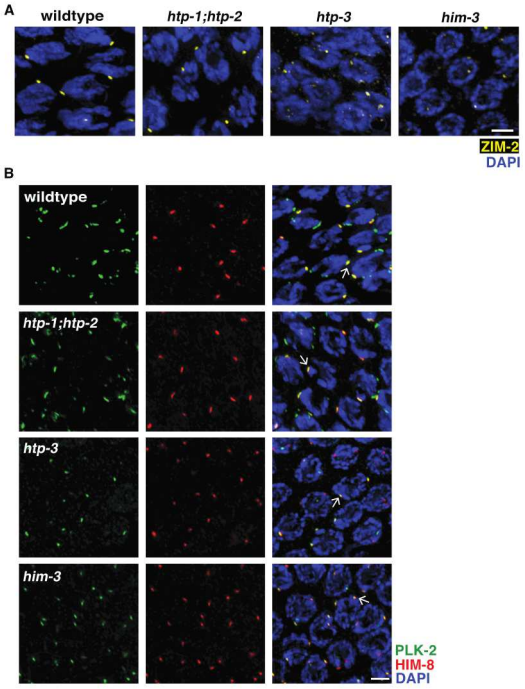

Figure 3-3: HTP-3 and HIM-3 disrupt localization of some but not all PC proteins. (A) Images of early meiotic prophase nuclei in wild-type worms, *htp-1/2, htp-3,* and, *him-3* mutants stained to visualize ZIM-2 (yellow) and DAPI (blue). (B) Images of early meiotic prophase nuclei in wild-type worms, *htp-1/2, htp-3,* and, *him-3* mutants stained to visualize PLK-2 (green), HIM-8 (red) and DAPI (blue). Arrows indicate an example of colocalization of PLK-2 and HIM-8. Scale bar represents 2 μm.

syp-3 mutants have active PCs

Similar to *htp-3*, *him-3* and *htp-1 htp-2* mutants, *syp-3* mutants have unsynapsed chromosomes but fail to elevate germline apoptosis in response to the synapsis checkpoint (Fig. 3-1 D). Unlike *htp-3*, *him-3* and *htp-1 htp-2* mutants, *syp-3* mutants display a delay in meiotic progression (Smolikov et al., 2007), likely because HTP-3, HIM-3, HTP-1 and HTP-2 are present to promote this delay (Kim et al., 2015). However, this delay in meiotic progression does not depend on PC function (Kim et al., 2015), raising the possibility that *syp-3* mutants abrogate the synapsis checkpoint due to defective PCs. To directly test this, we localized PLK-2 in meiotic prophase in *syp-3* mutants and compared them to wild-type

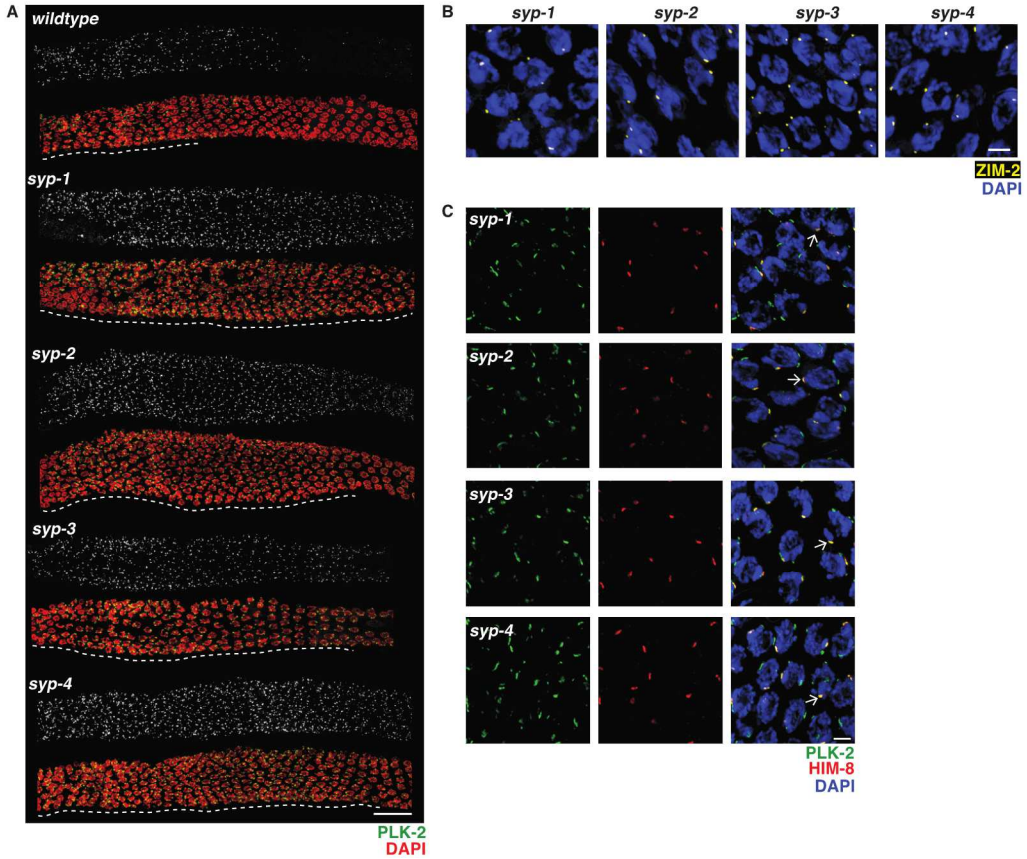

Figure 3-4: *syp-3* mutants have active PCs. (A) Images of germlines, from entry into meiosis until late meiotic prophase, of wild-type worms, *syp-1*, *syp-2, syp-3*, and *syp-4* mutants stained to visualize PLK-2 (green and grayscale) and DAPI (red). Delay in meiotic progression indicated by white dashed line. Scale bar represents 30 µm. (B) Images of early meiotic prophase nuclei in wild-type worms, *syp-1*, *syp-2, syp-3*, and *syp-4* mutants stained to visualize ZIM-2 (yellow) and DAPI(blue). (C) Images of early meiotic prophase nuclei in wild-type worms, *syp-1*, *syp-2, syp-3*, and *syp-4* mutants stained to visualize PLK-2 (green), HIM-8 (red) and DAPI (blue). Arrows indicate an example of colocalization of PLK-2 and HIM-8. Scale bar represents 2 µm.

worms, *syp-1*, *syp-2* and *syp-4* mutants. Similar to wild-type animals and *syp-1* (Harper et al., 2011) (Labella et al., 2011), *syp-2* and *syp-4* mutants, *syp-3* mutants robustly localized PLK-2 to PCs (Figure 4A). Moreover, unlike wild-type germlines, PLK-2 localization is extended on PCs in *syp-3* mutants, similar to *syp-1*, *syp-2* and *syp-4* mutants (Fig. 3-4 A).

We complemented this evaluation of PC function by localizing ZIM-2 and HIM-8 in *syp-3* mutants and compared this to *syp-1*, *syp-2* and *syp-4* mutants. ZIM-2 forms robust patches in meiotic nuclei in *syp-3* mutants, similar to *syp-1, 2 and 4* mutants (Fig. 3-4 B). Furthermore, HIM-8 localizes to all meiotic nuclei in *syp-3* mutants and co-localizes with PLK-2 (Fig. 3-4 C). These data show that SYP-3 is required for the synapsis checkpoint in a mechanism distinct from regulating PC function.

Altogether, our data show that some SC components, namely SYP-3, HTP-3, HIM-3 and HTP-1, are required for the synapsis checkpoint. Therefore, we suggest that the synapsis checkpoint may monitor some aspects of SC assembly to prevent aneuploid gametes from being produced. Uncovering which specific functions of SYP-3 and the HORMADs are required for the synapsis checkpoint are intriguing questions to be addressed in future studies.

Surprisingly, despite having similar defects in synapsis, we found that not all central element components of the SC are equivalent in the context of checkpoint function. While *syp-2* mutants essentially phenocopy *syp-1* mutants, *syp-4* mutants appear to have a functional synapsis checkpoint that is PCH-2 independent. We favor the interpretation that there may be differences in the genetic requirements for the synapsis checkpoint depending on what the checkpoint is responding to. Loss of PCH-2 stabilizes pairing in *syp-1* mutants (Deshong et al., 2014), leading us to hypothesize that this stabilization of pairing is what satisfies the synapsis checkpoint in *pch-2;syp-1* and *pch-2;syp-2* double mutants. Therefore, it is possible that this stabilization does not occur in *pch-2;syp-4* mutants, providing an explanation for why PCH-2 is not required for the synapsis checkpoint in *syp-4* mutants. Alternatively, SYP-4 could be playing another role during the synapsis checkpoint. SYP-4

was identified by virtue of its two-hybrid interaction with SYP-3. However, unlike SYP-3, SYP-4 does not show an interaction with either SYP-1 or SYP-2 by two-hybrid (Smolikov et al., 2009). While there are a variety of reasons why relevant protein-protein interactions might not be recapitulated by yeast two-hybrid assays, these negative data suggest that SYP-4 could uniquely interact with SYP-3 during synapsis. For example, one scenario consistent with our data is that when SYP-3 is not bound to SYP-4, SYP-3 signals to the synapsis checkpoint and when it is bound to SYP-4, this signal is silenced. Future experiments will address this hypothesis.

Materials and Methods

Genetics and Worm Strains

The wildtype *C. elegans* strain background was Bristol N2 (Brenner, 1974). All experiments were performed on adult hermaphrodites at 20° under standard conditions. Mutations and rearrangements used were as follows:

LG I: *htp-3(tm3655)*, *syp-4 (tm2713)*, *cep-1(gk138)*, *syp-3(ok258)*, *hT2 [bli-4(e937) let-?(q782) qIs48]* (I;III)

LG II: *pch-2(tm1458)*

LG IV: *htp-1(gk174)*, *htp-2(tm2543)*, *him-3(gk149)*, *spo-11(ok79)*, *nT1[unc-?(n754) let-?(m435)] (IV, V)*, *nT1 [qIs51]* (IV, V)

LG V: *syp-2(ok307), syp-1(me17), bcIs39(Pim::ced-1::GFP)*

Quantification of Germline Apoptosis

Scoring of germline apoptosis was performed as previously descried in (Bhalla and Dernburg, 2005). L4 hermaphrodites were allowed to age for 22 hours at 20°C. Live worms were mounted under coverslips on 1.5% agarose pads containing 0.2mM levamisole. A minimum of twenty-five germlines were analyzed for each genotype by performing live fluorescence microscopy and counting the number of cells fully surrounded by CED-1::GFP.

Significance was assessed using a paired t-test. All experiments were performed at least twice.

Antibodies, Immunostaining and Microscopy

Immunostaining was performed on worms 20 to 24 hours post L4 stage. Gonad dissection were carried out in 1X EBT (250 mM HEPES-Cl pH 7.4, 1.18 M NaCl, 480 mM KCl, 20 mM EDTA, 5 mM EGTA) + .1% Tween 20 and 20mM sodium azide. An equal volume of 2% formaldehyde in EBT (final concentration was 1% formaldehyde) was added and allowed to incubate under a coverslip for five minutes. The sample was mounted on HistoBond (75x25x1mm from Lamb) slides and freeze-cracked and incubated in methanol at -20^{O}C for one minute and transferred to PBST. Following several washes of PBST the samples were incubated for 30-min in 1% bovine serum albumin diluted in PBST. A hand-cut paraffin square was used to cover the tissue with 50 µL of antibody solution. Incubation was conducted in a humid chamber overnight at 4°C. Slides were rinsed in PBST, then incubated for 2 hours at room temperature with fluorophore-conjugated secondary antibody at a dilution of 1:500. The samples were then mounted in 13 ul of mounting media (20 M N-propyl gallate (Sigma) and 0.14M Tris in glycerol) with a No. 1 ½ (22mm^2) coverslip and sealed with nail polish.

Primary antibodies were as follows (dilutions are indicated in parentheses): guinea pig anti-ZIM-2 (1:2500) (Phillips and Dernburg, 2006), guinea pig anti-PLK-2 (1:750; (Harper, 2011 #18)) and rat anti-HIM-8 (1:250) (Phillips and Dernburg, 2006) Secondary antibodies were Cy3 anti-rabbit (Jackson Immunochemicals) and Alexa-Fluor 488 anti-guinea pig and anti-rat (Invitrogen).

All images were acquired at room temperature using a DeltaVision Personal DV system (Applied Precision) equipped with a 100X N.A. 1.40 oil-immersion objective (Olympus), resulting in an effective XY pixel spacing of 0.064 or 0.040 µm. Images were captured using a “camera” Three-dimensional image stacks were collected at 0.2-µm Z-spacing and processed

by constrained, iterative deconvolution. Imaging, image scaling and analysis were performed using functions in the softWoRx software package. Projections were calculated by a maximum intensity algorithm. Composite images were assembled and some false coloring was performed with Adobe Photoshop.

Bibliography

Akiyoshi, B., C.R. Nelson, J.A. Ranish, and S. Biggins. 2009. Quantitative proteomic analysis of purified yeast kinetochores identifies a PP1 regulatory subunit. *Genes & Development*. 23:2887-2899.

Albertson, D.G., A.M. Rose, and A.M. Villeneuve. 1997. Chromosome Organization, Mitosis, and Meiosis. *In C. elegans* II. D.L. Riddle, T. Blumenthal, B.J. Meyer, and J.R. Priess, editors. Cold Spring Harbor Laboratory Press, Plainview, NY. 47-78.

Aravind, L., and E.V. Koonin. 1998. The HORMA domain: a common structural denominator in mitotic checkpoints, chromosome synapsis and DNA repair. *Trends Biochem Sci*. 23:284-286.

Bader, J.R., and K.T. Vaughan. 2010. Dynein at the kinetochore: Timing, Interactions and Functions. *Semin Cell Dev Biol*. 21:269-275.

Baier, A., M. Alsheimer, and R. Benavente. 2007. Synaptonemal complex protein SYCP3: Conserved polymerization properties among vertebrates. *Biochim Biophys Acta*. 1774:595-602.

Bass, H.W., W.F. Marshall, J.W. Sedat, D.A. Agard, and W.Z. Cande. 1997. Telomeres cluster de novo before the initiation of synapsis: a three-dimensional spatial analysis of telomere positions before and during meiotic prophase. *J Cell Biol*. 137:5-18.

Basu, J., H. Bousbaa, E. Logarinho, Z. Li, B.C. Williams, C. Lopes, C.E. Sunkel, and M.L. Goldberg. 1999. Mutations in the essential spindle checkpoint gene bub1 cause chromosome missegregation and fail to block apoptosis in Drosophila. *J Cell Biol*. 146:13-28.

Basu, J., E. Logarinho, S. Herrmann, H. Bousbaa, Z. Li, G.K. Chan, T.J. Yen, C.E. Sunkel, and M.L. Goldberg. 1998. Localization of the Drosophila checkpoint control protein Bub3 to the kinetochore requires Bub1 but not Zw10 or Rod. *Chromosoma*. 107:376-385.

Baudat, F., K. Manova, J.P. Yuen, M. Jasin, and S. Keeney. 2000. Chromosome synapsis defects and sexually dimorphic meiotic progression in mice lacking Spo11. *Mol Cell*. 6:989-998.

Bernard, P., K. Hardwick, and J.P. Javerzat. 1998. Fission yeast bub1 is a mitotic centromere protein essential for the spindle checkpoint and the preservation of correct ploidy through mitosis. *J Cell Biol*. 143:1775-1787.

Bhalla, N., and A.F. Dernburg. 2005. A conserved checkpoint monitors meiotic chromosome synapsis in Caenorhabditis elegans. *Science*. 310:1683-1686.

Bhalla, N., and A.F. Dernburg. 2008. Prelude to a division. *Annu Rev Cell Dev Biol*. 24:397-424.

Bhalla, N., D.J. Wynne, V. Jantsch, and A.F. Dernburg. 2008. ZHP-3 acts at crossovers to couple meiotic recombination with synaptonemal complex disassembly and bivalent formation in C. elegans. *PLoS genetics*. 4:e1000235.

Biggins, S., and A.W. Murray. 2001. The budding yeast protein kinase Ipl1/Aurora allows the absence of tension to activate the spindle checkpoint. *Genes & development*. 15:3118-3129.

Bohr, T., C.R. Nelson, E. Klee, and N. Bhalla. 2015. Spindle assembly checkpoint proteins regulate and monitor meiotic synapsis in C. elegans. *J Cell Biol*. 211:233-242.

Brenner, S. 1974. THE GENETICS OF CAENORHABDITIS ELEGANS. *Genetics*. 77:71-94.

Burger, J., J. Merlet, N. Tavernier, B. Richaudeau, A. Arnold, R. Ciosk, B. Bowerman, and L. Pintard. 2013. CRL(2LRR-1) E3-ligase regulates proliferation and progression through meiosis in the *Caenorhabditis elegans* germline. *PLoS Genet*. 9:e1003375.

Cahill, D.P., C. Lengauer, J. Yu, G.J. Riggins, J.K. Willson, S.D. Markowitz, K.W. Kinzler, and B. Vogelstein. 1998. Mutations of mitotic checkpoint genes in human cancers. *Nature*. 392:300-303.

Caryl, A.P., S.J. Armstrong, G.H. Jones, and F.C. Franklin. 2000. A homologue of the yeast HOP1 gene is inactivated in the Arabidopsis meiotic mutant asy1. *Chromosoma*. 109:62-71.

Chan, G.K., S.A. Jablonski, V. Sudakin, J.C. Hittle, and T.J. Yen. 1999. Human BUBR1 is a mitotic checkpoint kinase that monitors CENP-E functions at kinetochores and binds the cyclosome/APC. *J Cell Biol*. 146:941-954.

Chan, G.K., B.T. Schaar, and T.J. Yen. 1998. Characterization of the kinetochore binding domain of CENP-E reveals interactions with the kinetochore proteins CENP-F and hBUBR1. *J Cell Biol*. 143:49-63.

Cheeseman, I.M., and A. Desai. 2008. Molecular architecture of the kinetochore-microtubule interface. *Nat Rev Mol Cell Biol*. 9:33-46.

Chen, R.H., A. Shevchenko, M. Mann, and A.W. Murray. 1998. Spindle checkpoint protein Xmad1 recruits Xmad2 to unattached kinetochores. *J Cell Biol*. 143:283-295.

Chen, R.H., J.C. Waters, E.D. Salmon, and A.W. Murray. 1996. Association of spindle assembly checkpoint component XMAD2 with unattached kinetochores. *Science*. 274:242-246.

Chikashige, Y., C. Tsutsumi, M. Yamane, K. Okamasa, T. Haraguchi, and Y. Hiraoka. 2006. Meiotic proteins bqt1 and bqt2 tether telomeres to form the bouquet arrangement of chromosomes. *Cell*. 125:59-69.

Cleveland, D.W., Y. Mao, and K.F. Sullivan. 2003. Centromeres and kinetochores: from epigenetics to mitotic checkpoint signaling. *Cell*. 112:407-421.

Colaiacovo, M.P., A.J. MacQueen, E. Martinez-Perez, K. McDonald, A. Adamo, A. La Volpe, and A.M. Villeneuve. 2003. Synaptonemal complex assembly in C. elegans is

dispensable for loading strand-exchange proteins but critical for proper completion of recombination. *Dev Cell*. 5:463-474.

Conrad, M.N., C.Y. Lee, J.L. Wilkerson, and M.E. Dresser. 2007. MPS3 mediates meiotic bouquet formation in Saccharomyces cerevisiae. *Proc Natl Acad Sci U S A*. 104:8863-8868.

Couteau, F., K. Nabeshima, A. Villeneuve, and M. Zetka. 2004. A component of C. elegans meiotic chromosome axes at the interface of homolog alignment, synapsis, nuclear reorganization, and recombination. *Curr Biol*. 14:585-592.

Couteau, F., and M. Zetka. 2005. HTP-1 coordinates synaptonemal complex assembly with homolog alignment during meiosis in C. elegans. *Genes Dev*. 19:2744-2756.

Couteau, F., and M. Zetka. 2011. DNA damage during meiosis induces chromatin remodeling and synaptonemal complex disassembly. *Dev Cell*. 20:353-363

Davis, L.I., and G. Blobel. 1986. Identification and characterization of a nuclear pore complex protein. *Cell*. 45:699-709.

Dernburg, A.F. 2001. Here, there, and everywhere: kinetochore function on holocentric chromosomes. *J Cell Biol*. 153:F33-38.

Dernburg, A.F., K. McDonald, G. Moulder, R. Barstead, M. Dresser, and A.M. Villeneuve. 1998. Meiotic Recombination in C. elegans Initiates by a Conserved Mechanism and Is Dispensable for Homologous Chromosome Synapsis. *Cell*. 94:387-398.

Derry, W.B., A.P. Putzke, and J.H. Rothman. 2001. Caenorhabditis elegans p53: Role in Apoptosis, Meiosis, and Stress Resistance. *Science*. 294:591-595.

Deshong, A.J., A.L. Ye, P. Lamelza, and N. Bhalla. 2014. A quality control mechanism coordinates meiotic prophase events to promote crossover assurance. *PLoS Genet*. 10:e1004291.

Di Giacomo, M., M. Barchi, F. Baudat, W. Edelmann, S. Keeney, and M. Jasin. 2005. Distinct DNA-damage-dependent and -independent responses drive the loss of oocytes in recombination-defective mouse mutants. *Proc Natl Acad Sci U S A*. 102:737-742.

Ding, X., R. Xu, J. Yu, T. Xu, Y. Zhuang, and M. Han. 2007. SUN1 is required for telomere attachment to nuclear envelope and gametogenesis in mice. *Dev Cell*. 12:863-872.

Dombecki, C.R., A.C. Chiang, H.J. Kang, C. Bilgir, N.A. Stefanski, B.J. Neva, E.P. Klerkx, and K. Nabeshima. 2011. The chromodomain protein MRG-1 facilitates SC-independent homologous pairing during meiosis in Caenorhabditis elegans. *Dev Cell*. 21:1092-1103.

Elowe, S., S. Hummer, A. Uldschmid, X. Li, and E.A. Nigg. 2007. Tension-sensitive Plk1 phosphorylation on BubR1 regulates the stability of kinetochore microtubule interactions. *Genes & development*. 21:2205-2219.

Essex, A., A. Dammermann, L. Lewellyn, K. Oegema, and A. Desai. 2009. Systematic analysis in Caenorhabditis elegans reveals that the spindle checkpoint is composed of two largely independent branches. *Mol Biol Cell*. 20:1252-1267.

Foley, E.A., and T.M. Kapoor. 2013. Microtubule attachment and spindle assembly checkpoint signalling at the kinetochore. *Nat Rev Mol Cell Biol*. 14:25-37.

Fraser, A.G., R.S. Kamath, P. Zipperlen, M. Martinez-Campos, M. Sohrmann, and J. Ahringer. 2000. Functional genomic analysis of C. elegans chromosome I by systematic RNA interference. *Nature*. 408:325-330.

Fraune, J., S. Schramm, M. Alsheimer, and R. Benavente. 2012. The mammalian synaptonemal complex: protein components, assembly and role in meiotic recombination. *Exp Cell Res*. 318:1340-1346.

Fukuda, T., K. Daniel, L. Wojtasz, A. Toth, and C. Hoog. 2010. A novel mammalian HORMA domain-containing protein, HORMAD1, preferentially associates with unsynapsed meiotic chromosomes. *Exp Cell Res*. 316:158-171.

Giroux, C.N., M.E. Dresser, and H.F. Tiano. 1989. Genetic control of chromosome synapsis in yeast meiosis. *Genome*. 31:88-94.

Goodyer, W., S. Kaitna, F. Couteau, J.D. Ward, S.J. Boulton, and M. Zetka. 2008. HTP-3 links DSB formation with homolog pairing and crossing over during C. elegans meiosis. *Dev Cell*. 14:263-274.

Hamill, D.R., A.F. Severson, J.C. Carter, and B. Bowerman. 2002. Centrosome maturation and mitotic spindle assembly in C. elegans require SPD-5, a protein with multiple coiled-coil domains. *Dev Cell*. 3:673-684.

Harper, N.C., R. Rillo, S. Jover-Gil, Z.J. Assaf, N. Bhalla, and A.F. Dernburg. 2011. Pairing centers recruit a Polo-like kinase to orchestrate meiotic chromosome dynamics in C. elegans. *Dev Cell*. 21:934-947.

Hassold, T., and P. Hunt. 2001. To err (meiotically) is human: the genesis of human aneuploidy. *Nat Rev Genet*. 2:280-291.

Herman, R.K., and C.K. Kari. 1989. Recombination between small X chromosome duplications and the X chromosome in Caenorhabditis elegans. *Genetics*. 121:723-737.

Hollingsworth, N.M., L. Goetsch, and B. Byers. 1990. The HOP1 gene encodes a meiosis-specific component of yeast chromosomes. *Cell*. 61:73-84.

Hua, S., R. Kittler, and K.P. White. 2009. Genomic antagonism between retinoic acid and estrogen signaling in breast cancer. *Cell*. 137:1259-1271.

Jin, D.Y., F. Spencer, and K.T. Jeang. 1998. Human T cell leukemia virus type 1 oncoprotein Tax targets the human mitotic checkpoint protein MAD1. *Cell*. 93:81-91.

Kim, Y., N. Kostow, and A.F. Dernburg. 2015. The Chromosome Axis Mediates Feedback Control of CHK-2 to Ensure Crossover Formation in C. elegans. *Dev Cell*. 35:247-261.

King, E.M., N. Rachidi, N. Morrice, K.G. Hardwick, and M.J. Stark. 2007. Ipl1p-dependent phosphorylation of Mad3p is required for the spindle checkpoint response to lack of tension at kinetochores. *Genes & development*. 21:1163-1168.

Kitagawa, R., and A.M. Rose. 1999. Components of the spindle-assembly checkpoint are essential in Caenorhabditis elegans. *Nat Cell Biol*. 1:514-521.

Kops, G.J., B.A. Weaver, and D.W. Cleveland. 2005. On the road to cancer: aneuploidy and the mitotic checkpoint. *Nat Rev Cancer*. 5:773-785.

Labella, S., A. Woglar, V. Jantsch, and M. Zetka. 2011. Polo kinases establish links between meiotic chromosomes and cytoskeletal forces essential for homolog pairing. *Dev Cell*. 21:948-958.

Labrador, L., C. Barroso, J. Lightfoot, T. Muller-Reichert, S. Flibotte, J. Taylor, D.G. Moerman, A.M. Villeneuve, and E. Martinez-Perez. 2013. Chromosome movements promoted by the mitochondrial protein SPD-3 are required for homology search during Caenorhabditis elegans meiosis. *PLoS Genet*. 9:e1003497.

Lake, C.M., and R.S. Hawley. 2012. The molecular control of meiotic chromosomal behavior: events in early meiotic prophase in Drosophila oocytes. *Annu Rev Physiol*. 74:425-451.

Li, Y., and R. Benezra. 1996. Identification of a human mitotic checkpoint gene: hsMAD2. *Science*. 274:246-248.

Li, X., and R.B. Nicklas. 1995. Mitotic forces control a cell-cycle checkpoint. *Nature*. 373:630-632.

Logarinho, E., H. Bousbaa, J.M. Dias, C. Lopes, I. Amorim, A. Antunes-Martins, and C.E. Sunkel. 2004. Different spindle checkpoint proteins monitor microtubule attachment and tension at kinetochores in Drosophila cells. *J Cell Sci*. 117:1757-1771.

Lui, D.Y., and M.P. Colaiacovo. 2013. Meiotic development in Caenorhabditis elegans. *Adv Exp Med Biol*. 757:133-170.

MacQueen, A.J., M.P. Colaiacovo, K. McDonald, and A.M. Villeneuve. 2002. Synapsis-dependent and -independent mechanisms stabilize homolog pairing during meiotic prophase in C. elegans. *Genes & development*. 16:2428-2442.

MacQueen, A.J., C.M. Phillips, N. Bhalla, P. Weiser, A.M. Villeneuve, and A.F. Dernburg. 2005. Chromosome Sites Play Dual Roles to Establish Homologous Synapsis during Meiosis in C. elegans. *Cell*. 123:1037-1050.

MacQueen, A.J., and A. Hochwagen. 2011. Checkpoint mechanisms: the puppet masters of meiotic prophase. *Trends Cell Biol*. 21:393-400.

Maresca, T.J., and E.D. Salmon. 2010. Welcome to a new kind of tension: translating kinetochore mechanics into a wait-anaphase signal. *J Cell Sci*. 123:825-835.

Martinez-Exposito, M.J., K.B. Kaplan, J. Copeland, and P.K. Sorger. 1999. Retention of the BUB3 checkpoint protein on lagging chromosomes. *Proc Natl Acad Sci U S A*. 96:8493-8498.

Martinez-Perez, E., M. Schvarzstein, C. Barroso, J. Lightfoot, A.F. Dernburg, and A.M. Villeneuve. 2008. Crossovers trigger a remodeling of meiotic chromosome axis composition that is linked to two-step loss of sister chromatid cohesion. *Genes Dev*. 22:2886-2901.

Martinez-Perez, E., and A.M. Villeneuve. 2005. HTP-1-dependent constraints coordinate homolog pairing and synapsis and promote chiasma formation during C. elegans meiosis. *Genes Dev*. 19:2727-2743.

Mercier, R., and M. Grelon. 2008. Meiosis in plants: ten years of gene discovery. *Cytogenet Genome Res*. 120:281-290.

Miki, F., K. Okazaki, M. Shimanuki, A. Yamamoto, Y. Hiraoka, and O. Niwa. 2002. The 14-kDa dynein light chain-family protein Dlc1 is required for regular oscillatory nuclear movement and efficient recombination during meiotic prophase in fission yeast. *Mol Biol Cell*. 13:930-946.

Murray, A.W. 1992. Creative blocks: cell-cycle checkpoints and feedback controls. *Nature*. 359:599-604.

Musacchio, A. and Salmon, E. D. 2007. The spindle-assembly checkpoint in space and time. *Nat Rev Mol Cell Biol*. 5:379-93.

Nezi, L., and A. Musacchio. 2009. Sister chromatid tension and the spindle assembly checkpoint. *Curr Opin Cell Biol*. 21:785-795.

Odorisio, T., T.A. Rodriguez, E.P. Evans, A.R. Clarke, and P.S. Burgoyne. 1998. The meiotic checkpoint monitoring synapsis eliminates spermatocytes via p53-independent apoptosis. *Nat Genet*. 18:257-261.

O'Rourke, S.M., M.D. Dorfman, J.C. Carter, and B. Bowerman. 2007. Dynein modifiers in C. elegans: light chains suppress conditional heavy chain mutants. *PLoS Genet*. 3:e128.

Ollinger, R., M. Alsheimer, and R. Benavente. 2005. Mammalian protein SCP1 forms synaptonemal complex-like structures in the absence of meiotic chromosomes. *Mol Biol Cell*. 16:212-217.

Page, S.L., and R.S. Hawley. 2004. The genetics and molecular biology of the synaptonemal complex. *Annu Rev Cell Dev Biol*. 20:525-558.

Penkner, A., L. Tang, M. Novatchkova, M. Ladurner, A. Fridkin, Y. Gruenbaum, D. Schweizer, J. Loidl, and V. Jantsch. 2007. The nuclear envelope protein Matefin/SUN-1 is required for homologous pairing in C. elegans meiosis. *Dev Cell*. 12:873-885.

Penkner, A.M., A. Fridkin, J. Gloggnitzer, A. Baudrimont, T. Machacek, A. Woglar, E. Csaszar, P. Pasierbek, G. Ammerer, Y. Gruenbaum, and V. Jantsch. 2009. Meiotic chromosome homology search involves modifications of the nuclear envelope protein Matefin/SUN-1. *Cell*. 139:920-933.

Phillips, C.M., and A.F. Dernburg. 2006. A family of zinc-finger proteins is required for chromosome-specific pairing and synapsis during meiosis in C. elegans. *Dev Cell*. 11:817-829.

Phillips, C.M., C. Wong, N. Bhalla, P.M. Carlton, P. Weiser, P.M. Meneely, and A.F. Dernburg. 2005. HIM-8 Binds to the X Chromosome Pairing Center and Mediates Chromosome-Specific Meiotic Synapsis. *Cell*. 123:1051-1063.

Pinsky, B.A., and S. Biggins. 2005. The spindle checkpoint: tension versus attachment. *Trends Cell Biol*. 15:486-493.

Pinsky, B.A., C. Kung, K.M. Shokat, and S. Biggins. 2006. The Ipl1-Aurora protein kinase activates the spindle checkpoint by creating unattached kinetochores. *Nat Cell Biol*. 8:78-83.

Roeder, G.S., and J.M. Bailis. 2000. The pachytene checkpoint. *Trends Genet*. 16:395-403.

Rog, O., and A.F. Dernburg. 2013. Chromosome pairing and synapsis during Caenorhabditis elegans meiosis. *Curr Opin Cell Biol*. 25:349-356.

Rog, O., and A.F. Dernburg. 2015. Direct Visualization Reveals Kinetics of Meiotic Chromosome Synapsis. *Cell Rep*.

Romanienko, P.J., and R.D. Camerini-Otero. 2000. The mouse Spo11 gene is required for meiotic chromosome synapsis. *Mol Cell*. 6:975-987.

Sato, A., B. Isaac, C.M. Phillips, R. Rillo, P.M. Carlton, D.J. Wynne, R.A. Kasad, and A.F. Dernburg. 2009. Cytoskeletal forces span the nuclear envelope to coordinate meiotic chromosome pairing and synapsis. *Cell*. 139:907-919.

Schild-Prufert, K., T.T. Saito, S. Smolikov, Y. Gu, M. Hincapie, D.E. Hill, M. Vidal, K. McDonald, and M.P. Colaiacovo. 2011. Organization of the synaptonemal complex during meiosis in Caenorhabditis elegans. *Genetics*. 189:411-421.

Shimanuki, M., F. Miki, D.Q. Ding, Y. Chikashige, Y. Hiraoka, T. Horio, and O. Niwa. 1997. A novel fission yeast gene, kms1+, is required for the formation of meiotic prophase-specific nuclear architecture. *Mol Gen Genet*. 254:238-249.

Schmekel K., Wahrman J., Skoglund U. and Daneholt B. 1993.The central region of the synaptonemal complex in *Blaps cribrosa* studied by electron microscope tomography.*Chromosoma.* 102: 669–681.

Schumacher, B., K. Hofmann, S. Boulton, and A. Gartner. 2001. The C. elegans homolog of the p53 tumor suppressor is required for DNA damage-induced apoptosis. *Current Biology*. 11:1722-1727.

Shonn, M.A., A.L. Murray, and A.W. Murray. 2003. Spindle checkpoint component Mad2 contributes to biorientation of homologous chromosomes. *Curr Biol*. 13:1979-1984.

Skoufias, D.A., P.R. Andreassen, F.B. Lacroix, L. Wilson, and R.L. Margolis. 2001. Mammalian mad2 and bub1/bubR1 recognize distinct spindle-attachment and kinetochore-tension checkpoints. *Proc Natl Acad Sci U S A*. 98:4492-4497.

Smolikov, S., A. Eizinger, K. Schild-Prufert, A. Hurlburt, K. McDonald, J. Engebrecht, A.M. Villeneuve, and M.P. Colaiacovo. 2007. SYP-3 restricts synaptonemal complex assembly to bridge paired chromosome axes during meiosis in Caenorhabditis elegans. *Genetics*. 176:2015-2025.

Smolikov, S., K. Schild-Prufert, and M.P. Colaiacovo. 2008. CRA-1 uncovers a double-strand break-dependent pathway promoting the assembly of central region proteins on chromosome axes during C. elegans meiosis. *PLoS Genet*. 4:e1000088.

Smolikov, S., K. Schild-Prufert, and M.P. Colaiacovo. 2009. A yeast two-hybrid screen for SYP-3 interactors identifies SYP-4, a component required for synaptonemal complex assembly and chiasma formation in Caenorhabditis elegans meiosis. *PLoS genetics*. 5:e1000669.

Shmoop Editorial Team. 2008. Mitosis. *Shmoop Biology*. Retrieved May 10, 2016, from http://www.shmoop.com/cell-cycle/mitosis.html

Shmoop Editorial Team. 2008. Meiosis. *Shmoop Biology*. Retrieved May 10, 2016, from http://www.shmoop.com/cell-cycle/meiosis.html

Starr, D.A., and J.A. Fischer. 2005. KASH 'n Karry: the KASH domain family of cargo-specific cytoskeletal adaptor proteins. *Bioessays*. 27:1136-1146.

Stein, K.K., E.S. Davis, T. Hays, and A. Golden. 2007. Components of the spindle assembly checkpoint regulate the anaphase-promoting complex during meiosis in Caenorhabditis elegans. *Genetics*. 175:107-123.

Stern, B.M., and A.W. Murray. 2001. Lack of tension at kinetochores activates the spindle checkpoint in budding yeast. *Curr Biol*. 11:1462-1467.

Stevens, D., K. Oegema, and A. Desai. 2013. Meiotic double-strand breaks uncover and protect against mitotic errors in the C. elegans germline. *Curr Biol*. 23:2400-2406.

Takeo, S., C.M. Lake, E. Morais-de-Sa, C.E. Sunkel, and R.S. Hawley. 2011. Synaptonemal complex-dependent centromeric clustering and the initiation of synapsis in Drosophila oocytes. *Curr Biol*. 21:1845-1851.

Tanneti, N.S., K. Landy, E.F. Joyce, and K.S. McKim. 2011. A pathway for synapsis initiation during zygotene in Drosophila oocytes. *Curr Biol*. 21:1852-1857.

Taylor, S.S., E. Ha, and F. McKeon. 1998. The human homologue of Bub3 is required for kinetochore localization of Bub1 and a Mad3/Bub1-related protein kinase. *J Cell Biol*. 142:1-11.

Tsai, J.H., and B.D. McKee. 2011. Homologous pairing and the role of pairing centers in meiosis. *J Cell Sci*. 124:1955-1963.

Tsubouchi, T., A.J. Macqueen, and G.S. Roeder. 2008. Initiation of meiotic chromosome synapsis at centromeres in budding yeast. *Genes & development*. 22:3217-3226.

Tsubouchi, T., and G.S. Roeder. 2005. A synaptonemal complex protein promotes homology-independent centromere coupling. *Science*. 308:870-873.

Villeneuve, A.M. 1994. A cis-acting locus that promotes crossing over between X chromosomes in Caenorhabditis elegans. *Genetics*. 136:887-902.

Waters, J.C., R.H. Chen, A.W. Murray, and E.D. Salmon. 1998. Localization of Mad2 to kinetochores depends on microtubule attachment, not tension. *The Journal of cell biology*. 141:1181-1191.

Woglar, A., A. Daryabeigi, A. Adamo, C. Habacher, T. Machacek, A. La Volpe, and V. Jantsch. 2013. Matefin/SUN-1 phosphorylation is part of a surveillance mechanism to coordinate chromosome synapsis and recombination with meiotic progression and chromosome movement. *PLoS Genet*. 9:e1003335.

Wojtasz, L., K. Daniel, I. Roig, E. Bolcun-Filas, H. Xu, V. Boonsanay, C.R. Eckmann, H.J. Cooke, M. Jasin, S. Keeney, M.J. McKay, and A. Toth. 2009. Mouse HORMAD1 and

HORMAD2, two conserved meiotic chromosomal proteins, are depleted from synapsed chromosome axes with the help of TRIP13 AAA-ATPase. *PLoS genetics*. 5:e1000702.

Wong, O.K., and G. Fang. 2007. Cdk1 phosphorylation of BubR1 controls spindle checkpoint arrest and Plk1-mediated formation of the 3F3/2 epitope. *The Journal of cell biology*. 179:611-617.

Wynne, D.J., O. Rog, P.M. Carlton, and A.F. Dernburg. 2012. Dynein-dependent processive chromosome motions promote homologous pairing in C. elegans meiosis. *The Journal of cell biology*. 196:47-64.

Yamamoto, T.G., S. Watanabe, A. Essex, and R. Kitagawa. 2008. SPDL-1 functions as a kinetochore receptor for MDF-1 in Caenorhabditis elegans. *The Journal of cell biology*. 183:187-194.

Yang, F., and P.J. Wang. 2009. The Mammalian synaptonemal complex: a scaffold and beyond. *Genome Dyn*. 5:69-80.

Ye, A.L., J.M. Ragle, B. Conradt, and N. Bhalla. 2014. Differential regulation of germline apoptosis in response to meiotic checkpoint activation. *Genetics*. submitted.

Zetka, M.C., I. Kawasaki, S. Strome, and F. Muller. 1999. Synapsis and chiasma formation in Caenorhabditis elegans require HIM-3, a meiotic chromosome core component that functions in chromosome segregation. *Genes Dev*. 13:2258-2270.

Zickler, D., and N. Kleckner. 2015. Recombination, Pairing, and Synapsis of Homologs during Meiosis. *Cold Spring Harb Perspect Biol*. 7.